eLife

Reviewed Preprint
v1 • October 14, 2025
Not revised

Reviewed Preprint
v2 • April 22, 2026
Revised by authors

For correspondence:
Krishnan_Padmanabhan@urmc.rochester.edu

Competing interests: No competing interests declared

Funding: See page 26

Reviewing editor: Tatyana O Sharpee, Salk Institute for Biological Studies, United States

Adult-neurogenesis allows for representational stability and flexibility in early olfactory system

Zhen Chen[1], **Krishnan Padmanabhan**[2]

[1]Department of Brain and Cognitive Sciences, University of Rochester, Rochester, United States • [2]Department of Neuroscience, University of Rochester School of Medicine and Dentistry, Rochester, United States

eLife Assessment

This paper presents an **important** theory and analysis of the role of neurogenesis and inhibitory plasticity in the drift of neural representations in the olfactory system. For one of the findings, regarding the impact of neurogenesis on the drift, the evidence remains **incomplete**. The reason lies in the differences in variability/drift of the mitral/tufted cell responses observed in the model compared to experimental observations, where these responses remain stable over extended time scales.

https://doi.org/10.7554/eLife.107905.2.sa3

Abstract

In the olfactory system, adult-neurogenesis results in the continuous reorganization of synaptic connections and network architecture throughout the animal's life. This poses a critical challenge: How does the olfactory system maintain stable representations of odors amidst this ongoing circuit instability? Utilizing a detailed spiking network model of early olfactory circuits, we uncovered dual roles for adult-neurogenesis: one that both supports representational stability to faithfully encode odor information and also one that facilitates plasticity to allow for learning and adaptation. In the main olfactory bulb, adult-neurogenesis affects neural codes in individual mitral and tufted cells but preserves odor representations at the neuronal population level. By contrast, in the olfactory piriform cortex, both individual cell responses and overall population dynamics undergo progressive changes due to adult-neurogenesis. This leads to representational drift, a gradual alteration in stimulus-evoked activity patterns. Both processes are dynamic and depend on experience such that repeated exposure to specific odors reduces the drift due to adult-neurogenesis; thus, when the odor environment is stable over the course of adult-neurogenesis, it is spike-timing-dependent plasticity that leads representations to remain stable in piriform cortex; when those olfactory environments change, adult-neurogenesis allows cortical representations to track environmental change. Whereas perceptual stability and plasticity due to learning are often thought of as two distinct, often contradictory processes in neuronal coding, we find that adult-neurogenesis serves as a shared mechanism for both. In this regard, the quixotic presence of adult-neurogenesis in the mammalian olfactory bulb that has been the focus of considerable investigation in chemosensory neuroscience may be the mechanistic underpinning behind an array of complex computations.

Introduction

In the rodent brain, the main olfactory bulb (MOB) is one of two regions where neurogenesis persists throughout the animal's lifetime [1]. Adult-born cells in the sub-ventricular zone migrate to the MOB, where nearly 95% differentiate into inhibitory adult-born granule cells (abGCs) forming reciprocal dendro-dendritic connections [2,3] with the principal excitatory cells of the MOB, the mitral and tufted (M/T) cells. M/T cells in turn relay the chemosensory information to the

downstream targets including the olfactory or piriform cortex (PCx) [4–6]. Although both the cellular composition and synaptic organization of this circuit undergo constant changes due to adult-neurogenesis [7], animals are nonetheless able to perform incredibly complex behavioral tasks related to the determination of odor identity and concentration, requiring that they maintain stable representations of odors. This raises two critical questions: Does the encoding of odors via patterns of neural activity throughout the early olfactory system undergo changes as a result of this ongoing plasticity, and if so, how? If changes in neural activity due to adult-neurogenesis percolate throughout early olfactory circuits, what computational principles allow the system to represent the same odor stably over time?

Previous studies have explored the plasticity at synapses between M/T cells and abGCs, particularly in relation to olfactory learning [8–10]. It is known that sensory experience influences the survival and synaptic turnover of abGCs with M/T cells [7,11], impacting both the normal activity of these cells [12] and animal's performance in odor discrimination tasks [13]. However, the implications of these local synaptic changes in the bulb on the downstream areas, including in the PCx, which is critical for olfactory perception and learning [14,15], remain largely unexplored.

The three-layer PCx is thought to be a region where the components of an odor are assembled into an olfactory percept or representation. Subsets of piriform cells (PCs) respond when multiple M/T cells are activated in complex temporal sequences [16–18]. A given population of M/T cells from a single glomerulus, a neuropil like structure where inputs from individual olfactory receptor neuron types converge [19,20], project randomly to a distributed array of PCs [4–6]. As odor information in PCx is coded for through the combinatorial activity of PCs [21,22] it is hypothesized that PCx is where stable representations of odors are maintained [23]. However, recent evidence is beginning to challenge this idea [24]. First, NMDA mediated long-term potentiation (LTP) in both afferent and associate fibers to PCx [25,26] is similar to that observed in the CA1 region of hippocampus. PCs thus undergo synaptic plasticity on scales observed in other regions where representations are not stable [27]. Second, recent studies examining the responses of PCs over months demonstrate that patterns of activity in both individual cells and populations of cells can drift over time [24]. This representational drift has led to the hypothesis that PCx, rather than being a primary sensory area, may be more like an association cortical region [28,29]. However, the mechanisms by which this drift in PCx occurs remain unknown.

One clue that adult-neurogenesis in MOB may be the mechanism underlying these diverse processes is that neurogenesis occurs on a similar time scale to the representational drift in PCx, and the turnovers of abGCs is highly experience dependent [9] which is also reflected in the PCx drift [24]. More frequent exposure to the same odor slows down the representational drift in PCx, while the drift rate increases again once this frequent exposure was halted [24].

We therefore hypothesized that the long-term plasticity conferred by adult-neurogenesis in MOB percolates through the olfactory system serving as the mechanism of representational drift in PCx. To test this hypothesis, we used a spiking neuronal network model that replicated the circuit architecture within and between the MOB and PCx, integrating both the ongoing network restructuring due to adult-neurogenesis and the short-term plasticity of abGCs. We found that adult-neurogenesis differentially modulated odor responses and representations in M/T cells in the MOB and PCs in PCx. While the MOB maintained stable population representations despite changes in individual M/T cell responses due to neurogenesis, the PCx shows variation at both individual and population levels, leading to representational drift. Furthermore, when we incorporated spike-timing-dependent plasticity (STDP) at the synapses on abGCs, repeated odor exposure stabilized the PCx representations resulting in a reduction in drift rate. Taken together, we identified how the rules of plasticity on short-term time scales such as STDP and long-term time scales like adult-neurogenesis allow networks to both preserve sensory representations in some circuits like the MOB, while allowing other representations to change like those in PCx. Our work reveals the nuanced role played by adult-neurogenesis in balancing stability and adaptability in the chemosensory system.

Results

Spiking network model of adult-neurogenesis in early olfactory system

To understand the functional role of adult-neurogenesis of GCs on the odor representations in both MOB and PCx, we used a detailed spiking neural model that recapitulates the circuit architecture and neural dynamics of the early olfactory system (Fig.1A1, Methods). To this, we added adult-neurogenesis, which we modeled as a process where a subset of granule cells are killed off and new granule cells are integrated into the network as abGCs (Fig.1A1) [7,30]. We modeled this process by reshuffling the synaptic weights of 10% of GCs in the network with the total number of GCs fixed. The reshuffled synaptic weights include the weights between these abGCs and M/Ts, abGCs and other GCs or short axon cells (SACs), and the top-down feedback projections from PCs to abGCs (Fig.1A2). These new synaptic weights for abGCs were sampled from the same distributions that generated the initial network model, such that although individual weight values and connectivity were being modulated, the total distribution of synaptic weights remain stable (Fig.1B2). We simulated a total of 11 days of neurogenesis from Day-0 and Day-10 by which point almost all GCs in the model have gone through adult-neurogenesis. Over the course, the synaptic weights between M/Ts and GCs, GCs/SACs and GCs, PCs and GCs were changed to match the observed changes in experiments (Fig.1B1-1B3, FigS1). Although the empirical rate of adult-neurogenesis has been found to vary in rodent depending on the measurement approach and the behavioral paradigms being used [31], we selected a rate of 10% for a reasonable computational time. Notably, changing this rate in our model only affected the scale of the observations without qualitatively changing the core results. These gradual changes in the network connectivity allowed us to probe the long-term effect of adult-neurogenesis on odor processing and the effect it had on modulating odor representations in MOB and PCx over time.

Odors drive coordinated activity in structures called glomeruli from which M/T cells receive their information about the odors. To match the glomerular activation patterns both in terms of the identify and onset timing in response to real odors [32–34], we generated a panel of 100 model odors where each one activated 6%~20% of the total 50 glomeruli in the model with different onset latencies (Fig.1C1, FigS1). Each model odor was presented during a 250ms time window (4Hz sniff), corresponding to a single sniff that is ethologically and behaviorally relevant time-scale for rodents [35–37]. Our generated panel of model odors spanned a wide range of similarities, ranging from distinct odor pairs with low pairwise correlations (see Methods) to highly similar odor pairs with high pairwise correlations (Fig.1C2). The input to our network, the model odors at the glomerular level, remained unchanged across simulated days consistent with previous observations of stable odor responses of glomeruli [38]. Using this experimental paradigm, we could study how the same odor inputs were differently encoded for over the course of adult-neurogenesis by both the principal cells in the main olfactory bulb and the piriform cortex[14,39].

Modulation of individual cell responses and preservation of population representations in MOB

First, we examined how adult-neurogenesis affected the responses of both individual M/T cells in the bulb and the population. We found that individual M/T cells changed their responses to the same odor across days due to adult-neurogenesis, with some cells decreasing the firing rate responses (Fig.2A1 top) while other cells increased the magnitude of their responses (Fig.2A2 bottom, Fig.S2), similar to what has been observed by others using calcium imaging of M/T cell activity [38,40]. These changes in gain are consistent with a model of normalization, wherein the firing of an individual neuron is modulated within a regime. Notably, individual M/T cell responses also exhibited some extent of variability across repeated presentations of the same odor within a single session (Fig. S2, error bars). This within-session variability occurs on a much shorter time scale than adult-neurogenesis and therefore cannot be attributed to it. We return to this point and its implications in the Discussion. However, when we examined the M/T responses

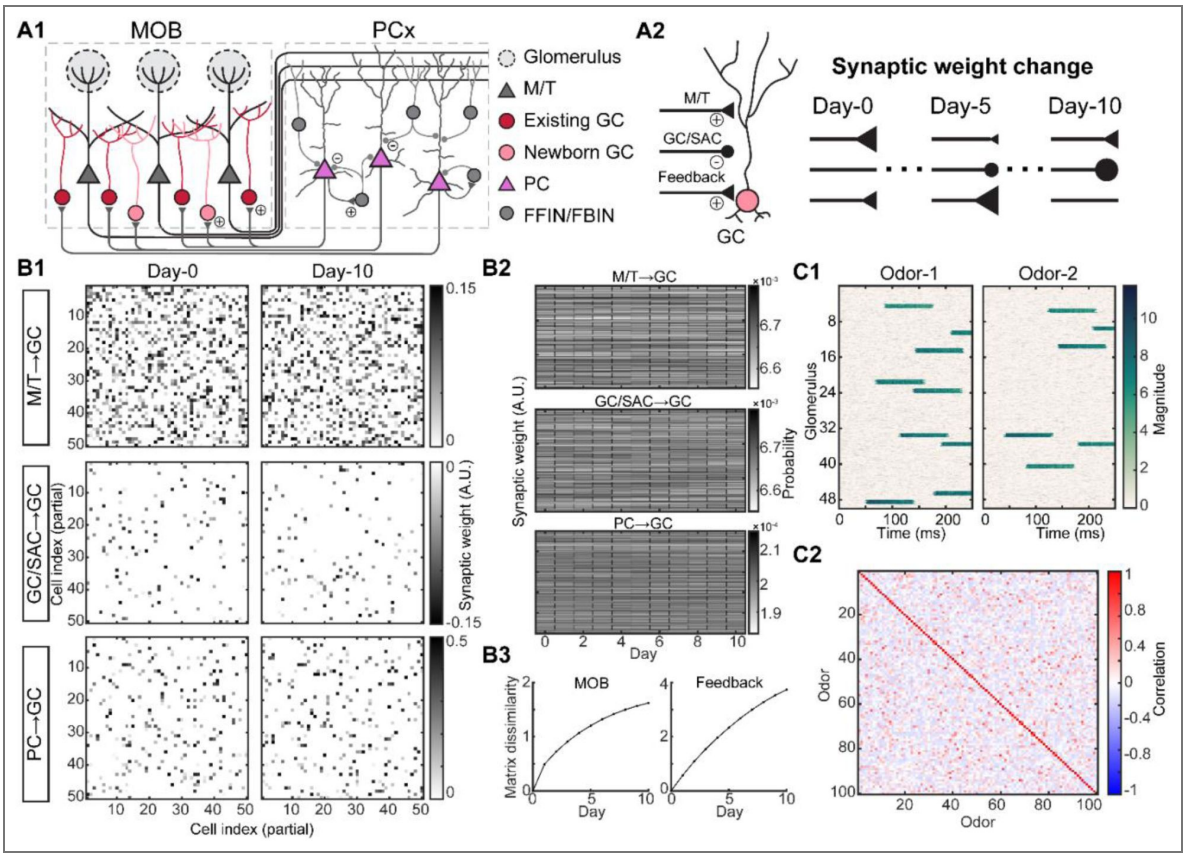

Figure 1. Spiking network model of adult-neurogenesis.

(A1). Schematic of early olfactory circuit. M/T: mitral/tufted cells, GC: granule cells, abGCs: adult-born GCs, PCs: piriform cortical cell, FFIN: feedforward inhibitory neuron, FBIN: feedback inhibitory neuron. Example plus signs indicate excitatory synapses and minus signs indicate inhibitory synapses. (A2). Schematic of synaptic reshuffling of GCs due to adult-neurogenesis. On each day, 10% of GCs have their weights reshuffled, including the synaptic weights from M/T cells, other GCs or short-axon cells (SAC), and PCs to GC (feedback). (B1). Partial weight matrix on two example days between GCs and M/T cells (top), other GCs or SACs (middle), and feedback from PCs (bottom). (B2). Histograms of all synaptic weights across days. (B3). Weight matrix dissimilarity between Day-0 and each other day. (C1). An example model odor generated by stimulating different combinations of glomerular identity and timing of activation. (C2). Pair-wise correlations between model odors show the relative similarities and differences across all model odors.

to the same odor across the population (Fig.2B2), we found that the overall pattern of population responses was preserved across days despite the ongoing neurogenesis. In this example, the odor activated 6 of the 50 glomeruli. Although individual M/T responses changed (Fig.2A1, **2A2** arrows), the groups of M/T cells driven by the same glomerulus preserved the temporal structure of their firing as a whole. Each individual M/T cell received certain amount of inhibition from a subset of GCs. With the incorporation of abGCs that eliminated some connections, and randomly established new ones, the synaptic weights of abGCs changed the inhibition at the individual M/T cell level, but preserved the distribution of inhibition across the population of M/T cells associated with each glomerulus. As a result, adult neurogenesis effectively preserved the ensemble response to each odor for M/T cells associated with a single glomerulus but led to a reshuffling of the identity of which M/T cells responded at what time epoch and with what magnitude.

Next, we wanted to quantify the changes in M/T odor response across days due to adult-neurogenesis. We took the odor-evoked firing rate over the 250ms window across all M/T cells as a high-dimensional ensemble vector and computed their correlation between Day-0 and each other day. We named this correlation as "*full-ensemble correlation*". Regardless of using either single-trial (Fig.2A3) or trial-averaged responses (Fig.2A4), the within-odor full-ensemble correlation decreased significantly over time. This decrease is consistent with experimental observations [40]. The across-odor correlations, computed from responses evoked by different odors, remained low across all days (Fig.2A4). Therefore, these results indicated that the gradual changes in the odor-evoked responses of individual M/T cells (Fig.2A1) accumulated over time.

However, as we observed above, the overall pattern of M/T population responses was preserved (Fig.2A2), suggesting that the covariance, a measure of the shared fluctuations across M/T population might remain stable. To test this, we projected M/T population responses into a low-dimensional space (Fig.2B1, **2B2,** see Methods), where the time varying odor-evoked responses across the population constituted a trajectory in the odor representation space of M/T cell population activity. For the two example odors, the M/T trajectories of the same odor stayed quite close on the two example days (Fig.2B1). If we simplified the single-trial trajectories by only plotting the maximal-distance points to the origin (Fig.2B2), we found that the points of the same odor (color) stayed clustered together in the space across all days (darkness of the color) despite the ongoing circuit restricting due to adult-neurogenesis. The correlation of the low-dimensional trajectories, which we named as "*reduced-space correlation*", remained high across all days (Fig.2B3), and only dropped to ~0.7-0.8 on Day-10 (Fig.2B4). This is consistent with a recent experimental study using calcium-imaging on M/T cells [41]. Additionally, while the authors [41], observed relative stability of odor responses in some of the individual M/T cells, they also observed that the full-ensemble showed a clear monotonic increase in response differences over a long time intervals of months. In this regard, our results showed that although adult-neurogenesis gradually varied the responses of individual M/T cells, the low-dimensional representations of M/T cells in the reduced space remained stable across days despite the changes in local synaptic organization due to adult-neurogenesis.

Modulation of both individual cell responses and population representations in PCx

M/T cells in MOB send random projections to PCx, such that each individual piriform cell receives input from a random subset of M/T cells associated with different glomeruli [4,6]. PCx cells incorporate this feedforward information about odor identity and concentration from the individual M/T cells in the MOB [14] and assembles those components into an olfactory percept [21,23]. Although perceptual stability is a hallmark of sensory processing and piriform cortex has historically been thought to be a place where perceptual stability is established in the population code, recent evidence has started to challenge this idea [24]. We hypothesized that the gradual changes in the individual M/T responses, passed through the nonlinearities of synaptic integration, would affect the responses of PCs at both individual and population level. We studied this by looking at the activity of individual PCs and the ensembles of PCs in PCx.

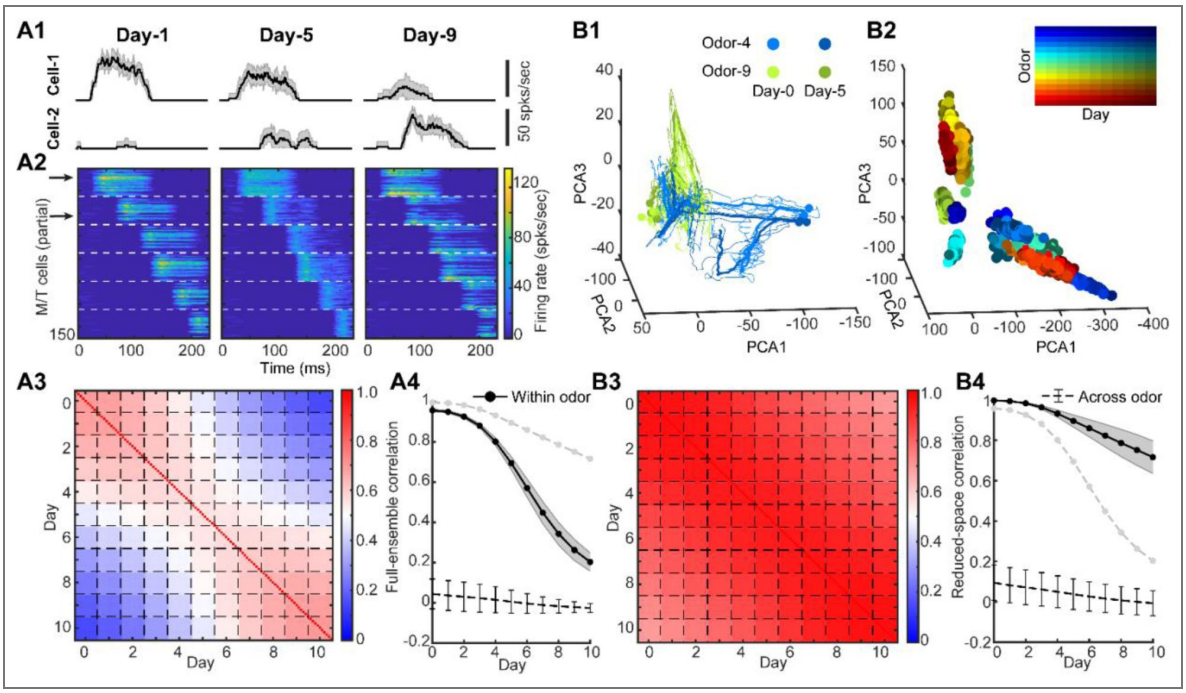

Figure 2. Adult-neurogenesis modulates individual M/T cell responses but preserves population representation.

(A1). Trail-averaged firing rate of two example M/T cells responding to the same odor (within-odor) on three different days (mean ± SD, n = 10 trials). (A2). Firing rate patterns of odor-activated M/T cells to the same odor on three days. M/T cells driven by different glomeruli are separated by white dashed line. The two arrows correspond to the two example cells in (A1). (A3). Pairwise within-odor full-ensemble correlation of single-trial M/T cell responses between each day averaged across all odors (n = 100). Each small box separated by the dashed lines is a 10×10 matrix (n = 10 trials) corresponding to autocorrelation (same day on diagonal) and cross-correlation (different days off diagonal). (A4). Full-ensemble correlation of trial-averaged M/T cell responses for within-odor (black solid line with error bar: mean ± SD, n = 100 odors).) and across-odor (black dashed line with error bar: mean ± SD, n = 10 pairs) between Day-0 and each other day. Grey dashed line with no error bar: same as the black solid line in (B4). (B1). Low-dimensional trajectories of M/T responses to two example odors (color) on two different days (darkness of color). Thin curves: single-trial trajectories, thick curves: trial-averaged trajectories, points: maximal-distance points on trajectory to the origin. (B2). Only maximal-distance points are shown for different odors on different days. (B3). Similar to (A3) but for reduced-space correlation computed using the low-dimensional M/T trajectories (single-trial). (B4). Similar to (A4) but for reduced-space correlation computed using the low-dimensional M/T trajectories (trial-averaged). Grey dashed line with no error bar: same as the black solid line in (A4).

Like M/T cells, the responses of individual PCs to the same odor varied across days. Some PCs increased their responses while others decreased responses (Fig.3A1, Fig.S3), consistent with recent chronic recordings in PCx (Fig.S4) [24]. However, unlike M/T cells, the overall pattern of PCs responses varied as a result of adult-neurogenesis (Fig.3A2). Some PCs responding strongly on Day-1 became inactive on Day-9, whereas some PCs that did not respond on Day-1 became strongly activated on Day-9. Consequently, the combinatorial patterns of activated PCs by the same odor were reorganized by adult-neurogenesis on different days. Additionally, we also found that the temporal structure of firing rate in individual PCs was highly variable. For example, some PCs changed the onset and duration of their activation over the course of neurogenesis (Fig.3A2). As a consequence, the within-odor full-ensemble correlation showed a significant drop for PCs (Fig.3A3, **3A4**). This is consistent with recent studies examining the responses of PCs over time and demonstrating that patterns of PCs responses in both individual cells and populations of cells can *drift* over time [24].

Changes in the firing rates reflect the changes in the variance of individual cells (Fig.S5), but they do not say anything about the covariance, nor do they capture the nonlinear interactions that shape the representations in PC populations when synaptic information is integrated across M/T cell inputs and passes through the threshold nonlinearity in individual PCs reflective of this integration. To study this, we calculated the covariance across population of PCs was impacted by adult-neurogenesis. In contrast to the M/T population where the representational trajectories of the same odor followed one another closely in the space across different days, we found that the low-dimensional trajectories of PCs showed a large variability across different days (Fig.3B1). As a result, the maximal-distance points for the trajectories on each day were broadly spread in the space across progressive days of neurogenesis (Fig.3B2). These results are consistent with representational drift in the odor encoding space. Quantitatively, the within-odor reduced-space correlation decreased substantially across days (Fig.3B3, **3B4**). Our data suggests that as a consequence of both the random projections of M/T cells to different PCs and the ways in which the cortical cells integrate those inputs, PCx representations drift with ongoing adult neurogenesis in the bulb.

Next, we asked how adult-neurogenesis geometrically reshaped the odor manifold and representational trajectories in the high-dimensional space? Recent computational models that have been built on longstanding frameworks of population coding suggest that neural representations reside in a high-dimensional manifold [42,43]. First, we reasoned that the structure of the odor manifold would be defined as the aggregation of the odor-evoked temporal responses within a sniff cycle to all the odors based on evidence showing that different odors evoke complex and distinct temporal activities in both M/T cells [44–46] and PCs [47–49]. For visualization, we plotted the odor manifold in the three-dimensional PCA space (Fig.S6). We found the odor manifolds of M/T cells were highly overlapping with each other, whereas for PCs they were much more separated. Across individual odors, we quantified the geometrical reshaping of representational trajectories by calculating the cosine similarity (see **Methods**) which measures the similarity between two vectors. It has a value 1 if the two vectors have the same direction, and a value 0 if they are orthogonal. We found that cosine similarity using the population firing rate of M/T cells and PCs had a similar degree of decrease as the function of intervals (i.e., number of days between two representations) (Fig.S7A1). However, the cosine similarity using representational trajectories remained stable for M/T cell but reduced for PCs (Fig.S7B1).

If representations drift as a result of adult-neurogenesis, then behaviors too should be impacted, drifting in a similar timescale. To unpack this connection, we used the K-nearest neighbor algorithm as the decoder (see **Methods**). We found that the decoding accuracy for discriminating against two different odors using M/T cell population responses was high but accuracy in PCs dropped substantially capturing the representational flexibility in PCx (Fig.S7).

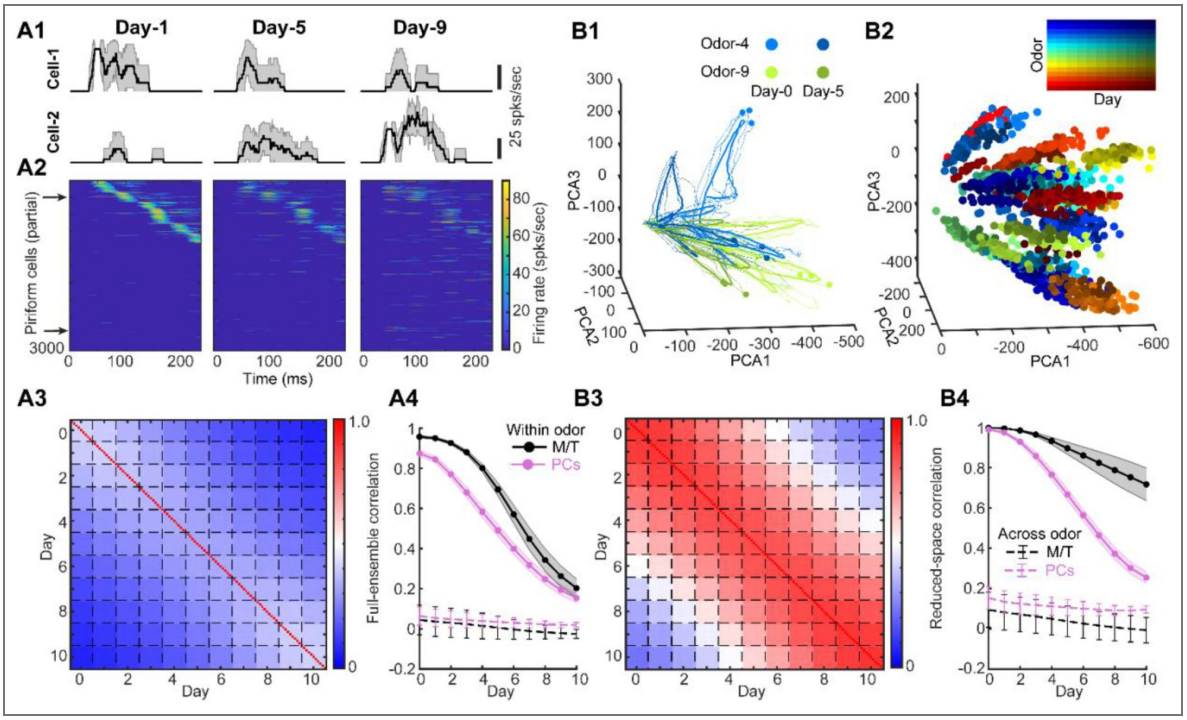

Figure 3. Adult-neurogenesis modulates both individual PCs responses and population representations.

(A1). Trail-averaged firing rate of two example PCs responding to the same odor on three different days (mean ± SD, n = 10 trials). (A2). Firing rate patterns of partial PCs responding to the same odor on three days. The two arrows correspond to the two example cells in (A1). (A3). Pairwise within-odor full-ensemble correlation of single-trial PCs responses between each day averaged across all odors (n = 100). Each small box separated by the dashed lines is a 10×10 matrix (n = 10 trials) corresponding to autocorrelation (same day on diagonal) and cross-correlation (different days off diagonal). (A4). Full-ensemble correlation of trial-averaged cell (PCs: purple; M/T: black) responses for within-odor (solid line with error bar: mean ± SD, n = 100 odors).) and across-odor (dashed line with error bar: mean ± SD, n = 10 pairs) between Day-0 and each other day. The curves for M/T cells are the same lines as in Fig.2. (B1). Low-dimensional trajectories of PCs responses to two example odors (color) on two different days (darkness of color). Thin curves: single-trial trajectories, thick curves: trial-averaged trajectories, points: maximal-distance points on trajectory to the origin. (B2). Only maximal-distance points are shown for different odors on different days. (B3). Similar to (A3) but for reduced-space correlation computed using the single-trial PCA trajectories of PCs. (B4). Similar to (A4) but for reduced-space correlation computed using the trial-averaged PCA trajectories of PCs.

Experience-dependent plasticity enhances representational stability in PCx

So far, we have shown that adult-neurogenesis, a process that changes the circuit structure of the early olfactory system, is one mechanism by which representational drift in PCx happens. Interestingly, it has been reported that repeated experience of an odorant stabilizes odor representations and thus reduces the drift in PCx [24]. The mechanism which drives drift also appears to stabilize that drift when the olfactory environment is stable, suggesting that a core feature of the mechanism should be plasticity. Since the synapses of abGCs have been shown to be highly plastic and experience-dependent [8,9,50], we reasoned that experience-dependent plasticity of the same abGCs that drive representational in PCx may also stabilize that drift in response to the experience of encountering a stable olfactory environment.

To model experience-dependent changes at the level of synapses, we implemented a spike-timing-dependent plasticity (STDP) rule [51–53] across the diversity of the synapses related to an abGC (Fig.4A1). Depending on the spike timing interval of pre- and post-synaptic neurons, the synaptic weight could be either facilitated or suppressed (Fig.4A2, see Methods). Experience then was modeled as repeated presentations of the same set of odors every day (50 trials for each odor per day) to our network model, while adult-neurogenesis was occurring as previously described, with the network presumably learning these stable representations in the pattern of synaptic connectivity. In this example GC, the adult-neurogenesis that took place on day-4, resulted in a new cell being added to the circuit, while the existing cell was removed, a process that randomly reset a group of synaptic weights (say, S1 and S2, Fig.4B) across two days of neurogenesis. Without STDP, the synaptic weights S1 and S2 would keep constant or fluctuate by some stochastic process, regardless of what was happening in the environment, including the effects of the repeated experience of an odor (black line, Fig.4B). The implementation of STDP meant that the synaptic weight may change on a trial-by-trial basis when an odor was repeatedly presented (blue line, Fig.4B). In the end, the weight S1 may be enhanced while the weight S2 may be suppressed. Although odor representations of M/T cells remained stable with and without STDP (Fig.4C1), we found that odor representations in PCx were stabilized with STDP (Fig.4C2). The correlation drops from day-0 were significantly reduced (0.8 without STDP and 0.4 with STDP by day-10, Fig.4C2 left), and the drift rate (° per day), which quantified the daily angle changes of the population responses (see **Methods**), was reduced by 26% (7.9 without STDP and 5.8 without STDP, Fig.4C2 right). Adding STDP to the network and using repeated presentations of an odor meant that the synapses that would otherwise randomly change due to adult-neurogenesis converged asymptotically to some weight (Fig.S8). Importantly, we identified that while the brain is constantly undergoing change, especially in the MOB and the PCx due to ongoing adult-neurogenesis, the impact of these changes on both population responses and the representation depends as much on the plasticity rules as it does on the ongoing statistics of the environment.

Discussion

In our study, we modeled adult-neurogenesis as a dynamic reshuffling of granule cells (GCs) within a detailed spiking neuronal network that replicated the circuit architecture of the main olfactory bulb (MOB) and piriform cortex (PCx). This modeling revealed how adult-neurogenesis differentially modulates odor responses and representations in mitral and tufted (M/T) cells and PCs.

In the MOB, individual M/T cells exhibited variable odor responses with changing firing rate magnitudes over time. This is consistent with earlier experimental studies using calcium-imaging [38,40,41]. Variability in M/T cell responses arises on multiple time scales. Experimental studies show pronounced trial-to-trial variability within single recording sessions [37,54–58], which cannot be attributed to adult-neurogenesis. This fast variability likely reflects ongoing network dynamics [59], behavioral state [38,60,61], attention [62], or top-down modulation [48,63,64], none of which are included in our model. Our model therefore captures only a limited amount of within-session variability and instead focuses on slower changes that accumulate across days. In this regime, adult-

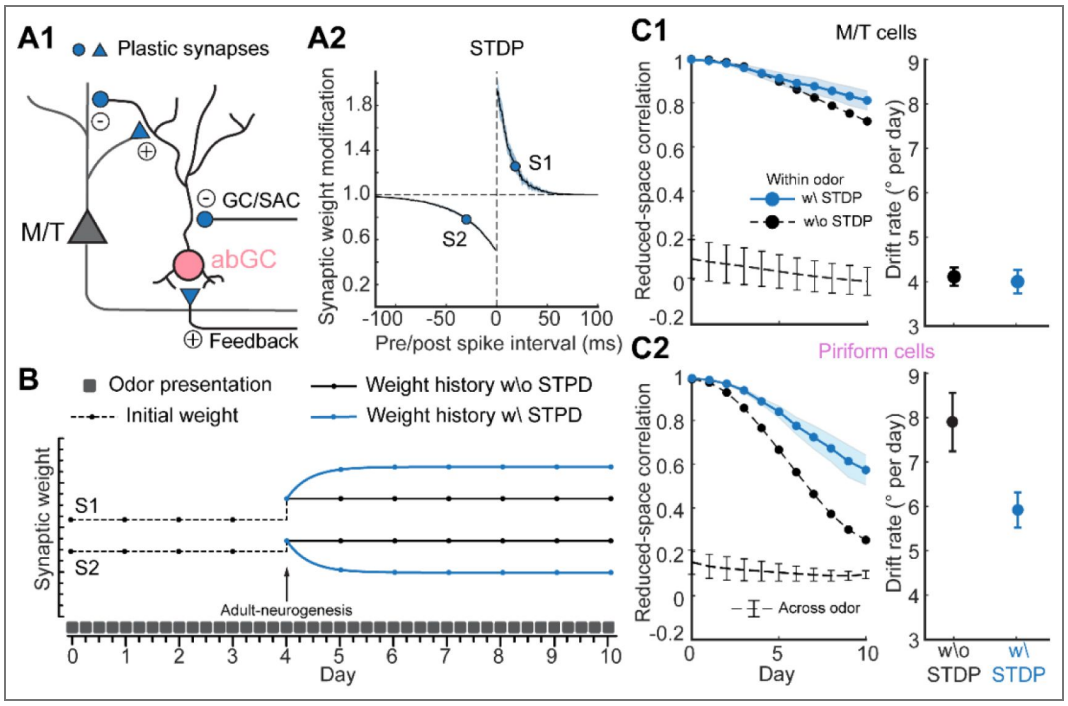

Figure 4. Experience-dependent plasticity enhances representational stability in PCx.

(A1). Different types of plastic synapses (blue) related to an abGC. Circle: inhibitory; triangle: excitatory. (A2). Dependence of synaptic modification on pre/post inter-spike interval used for the spike-timing-dependent plasticity (STDP). S1 and S2 are two example synapses with different modification – S1: facilitated; S2: suppressed. (B). Weight history of the two example synapses in A2 when an odor is repeatedly presented. Adult-neurogenesis happens on day-4 which randomly resets the weights. The synaptic weights stay constant without plasticity (black) while change trial by trial with plasticity (blue). (C1). Left: reduced-space correlation of trial-averaged M/T trajectories between Day-0 and each day. Blue solid line with error bar: within-odor and with STDP (mean ± SD, n = 10 odors); black dashed line without error bar: within-odor and without STDP. Black dashed line with error bar: across-odors, mean ± SD, n = 10 pairs. Right: drift rate for M/T trajectories with and without STDP. (C2). Same as C1 but for PCs trajectories.

neurogenesis provides a mechanism for gradual changes in individual M/T responses. It would be interesting for future work to integrate both fast and slow sources of variability within a unified modeling framework.

Despite these fluctuations in individual cells, the overall pattern of M/T cells population responses remained stable. This stability is attributed to consistent glomerular input, as reflected in the low-dimensional M/T cell trajectories and their proximity in reduced PCA space. This stability of M/T cells we observed in the reduced space is consistent with a recent experimental study [41] using both linear (PCA) and nonlinear (t-SNE) dimensionality reduction methods. Prior experimental studies report heterogeneous effects of experience on mitral cell odor responses. Repeated odor exposure has been associated with increased sparsening and reduced response amplitude in some experiments [38], whereas others report substantial reorganization of ensemble representations across days without consistent sparsening [40]. Our model best recapitulates the findings of the latter, showing that adult-neurogenesis can reorganize individual M/T responses while preserving stable low-dimensional population structure. Differences in behavioral features across studies may reflect variations in behavioral context or top-down modulation, factors that are not explicitly modeled here.

Conversely, in the PCx, both individual and population patterns of PCs responses were in constant flux due to the ongoing adult-neurogenesis. This resulted in a geometric reshaping of odor representations and a drift in the odor manifold defined by those representations, consistent with experimental finding[24]. Our results reveal how the process of adult-neurogenesis may support a number of computations in the early olfactory circuits, including how a sensory representation may remain stable, and how it might change due to plasticity.

We note that our simulations do not assume complete replacement of the granule cell population over the 11-day period. Rather, each simulated “day” represents a discrete epoch used to implement plasticity across multiple time scales. While some developmentally born granule cells can persist for much of the animal’s lifetime [65], some fraction of the population undergoes turnover through adult neurogenesis [7,66,67]. In our model, turnover is applied uniformly across granule cells, without preferential survival. Additionally, different simulated time points may also be thought of as reflecting regimes ranging from higher turnover to partial preservation of existing granule cells. While behavioral factors such as novelty or running can modulate neurogenesis rates [68–70], these effects are not included in our study and would be important for future studies.

Second, we found that one of the roles for STDP in the early olfactory system is reducing representational drift in the PCx. Repeated exposure to an odor significantly reduced the representational drift in the PCx, consistent with experimental observations[24]. Rather counterintuitively, this result suggests that a role of STDP and plasticity in general is stabilizing representations despite ongoing changes in the circuit. This implicates STDP at abGC-related synapses in a broader functional context. Previous experimental studies have shown that abGCs integrate into the olfactory bulb in an activity-dependent manner and preferentially stabilize circuits engaged by behaviorally relevant odors [9,50,71]. Our model is consistent with this view, but approaches the problem at the level of synaptic plasticity rather than cell survival. We show that STDP acting on abGC synapses can reduce representational drift by selectively stabilizing dimensions of population activity that are repeatedly activated due to experience. Here, representational stability arises because of the stability of the sensory world; Representational permanence, rather than being a feature of the circuit, is a feature of the sensory landscape, a stabilizing force against the inherent variability introduced by continuous adult neurogenesis. Adult-neurogenesis, which occurs throughout the animal’s life, may confer a mechanistically different computational framework as compared to vision or audition, for which critical periods delineate the bounds of plasticity, and define the periods over which sensory representations are changed or stabilized.

Third, our various dimensionality reduction analyses aim to illustrate the structure of population activity in terms of the variance and covariance of neuronal responses; which features of this activity are most relevant likely depend on what downstream brain regions receive this input and

what computations these regions ultimately perform. In this framework, both low and high-dimensional representations would be functionally relevant but may serve different roles. In the bulb, the low-dimensional population structure remains stable despite ongoing reorganization in the full ensemble, consistent with its role in providing a reliable sensory code. In contrast, PCx exhibits drift even in its low-dimensional space, reflecting its more flexible and higher-dimensional representational geometry. This higher dimensionality arises from divergent bulb inputs, dense recurrent connectivity, and integration of contextual and feedback signals. Importantly, STDP reduces drift in piriform cortex by stabilizing the dimensions reinforced by experience. Residual drift persists because the cortical population retains many orthogonal dimensions through which representations can continue to evolve.

Fourth, our model assumes broadly distributed projections from MOB to PCx and random intra-piriform connectivity [22,28,72]. These divergent projections from MOB to PCx is central to the combinatorial coding strategy of PCx, allowing individual pyramidal neurons to represent complex mixtures and higher-order odor features [14,73,74]. On the other hand, recent studies have revealed increasing structure in olfactory connectivity, including molecularly defined projection neuron subtypes, long-range functional loops, and experience-dependent motifs within piriform cortex [75–77]. These findings point to additional constraints that may shape learning and perception. An important direction for future work will be to incorporate such structured connectivity and cortical plasticity into our model to examine how they interact with adult-neurogenesis in the bulb to influence representational drift in PCx.

In addition to PCx, M/T cells also project to other cortical areas such as the anterior olfactory nucleus (AON). Although our model does not differentiate between mitral and tufted cells, it has been recently reported that mitral and tufted cells have distinct preferred cortical targets, with mitral cells preferentially projecting to PCx and tufted cells preferentially projecting to AON [75]. Tufted cells substantially outperform mitral cells in decoding both odor identity and intensity, suggesting that tufted cells and the AON where they project to are ideal for stably odor identity than the mitral cells and PCx [75]. As mitral cells are located in the deeper layers of the bulb, they interact with abGCs, whereas tufted cells in the superficial layer may preferentially interact with existing GCs that were born in the neonatal period [78,79]. Therefore, the activity of mitral cells may be more impacted by the turn-overs of abGCs, and the effect of adult-neurogenesis percolates onto PCx. By contrast, adult-neurogenesis has less impact on the tufted cells and the AON, potentially contributing to the stable encoding of odors in AON. This is one prediction of our model.

While our study focused on the effects of adult-neurogenesis in the olfactory bulb on odor representations, it does not negate the possibility of other forms of plasticity [80] contributing to the representational drift observed in the PCx [24]. Indeed, similar representational drifts have been noted in other brain areas like the posterior parietal cortex (PPC) [81], primary motor cortex [82], and hippocampus [83,84]. Of these regions, adult-neurogenesis only occurs in the hippocampus, where adult-born granule cells integrate into the existing circuitry of dentate gyrus [85]. Interestingly, similar to what we found in the early olfactory system (i.e., new-born cells in MOB and drift in PCx), the cells downstream of the dentate in the CA3 region [86] and CA1 region [27,83,84] exhibit drift over days and weeks. Both PCx and hippocampus are evolutionarily old archi-cortical structures. This conservation of adult-neurogenesis in these brain regions may suggest a broader evolutionary strategy for balancing stability and flexibility. First, adult-neurogenesis in the olfactory bulb may support ongoing plasticity due to continuous peripheral turnover of olfactory receptor neurons [7,87]. In this context, abGCs may provide a mechanism for adapting bulb circuitry to changing input statistics, injury, or learning demands. Second, adult-neurogenesis may confer selective advantages for navigating dynamic environments. By ensuring flexibility in neural circuits, such as through adult-neurogenesis, these regions can rapidly update the representations of odors and spatial information, respectively, in response to changing environmental cues. This flexibility may enable the early organisms to effectively represent and adapt to the dynamic worlds they inhabited, enhancing their chances of survival and reproduction across evolutionary time scales [90–92]. As organisms evolved, evolutionarily newer brain regions such as the PPC,

lacking significant adult-neurogenesis, developed alternative mechanisms to balance plasticity and stability [80]. Our work thus offers a new perspective on how the brain adapts to an ever-changing sensory environment.

Methods

Organization and architecture of the model

The MOB consisted of 50 glomeruli (G) corresponding to the olfactory receptor neuron (ORN) inputs into the MOB [19]. Each glomerulus was connected to 25 mitral/tufted (M/T) cells for a total 1250 M/T cells. Within the MOB, a local population of 12,500 inhibitory granule cells (GCs) formed reciprocal and lateral inhibitory connections with M/T cells. Individual M/T cell "projections" formed random excitatory connections with 10,000 piriform cortical cells (PCs) in PCx. These PCs in turn "projected" back to the olfactory bulb, provided excitatory centrifugal feedback onto the inhibitory granule cells in the bulb. Within PCx, two types of inhibitory interneurons were included: a population of 1250 feedforward inhibitory neurons (FFIs) that received excitatory input from M/T cells and inhibited both PCs and other FFIs, and a population of 1250 local feedback inhibitory neurons (FBIs) that received input from a random subset of PCs and subsequently inhibited PCs and other FBIs.

Voltage dynamics of individual neurons

The voltage dynamics of individual cells in the network are modeled as spiking neurons [93] described by a two-dimensional (2D) system of ordinary differential equations of the form,

$$\begin{aligned} \frac{dv}{dt} &= 0.04v^2 + 5v + 140 - u + I \\ \frac{du}{dt} &= a(bv - u) \end{aligned} \tag{1}$$

with the after-spiking resetting

$$\text{if } v \geq 30\,\text{mV}\,,\ \text{then } v \leftarrow c, u \leftarrow u + d \tag{2}$$

Here v represents the voltage (mV) of the neuron and u represents a dimensionless membrane recovery variable accounting for the activation or inactivation of ionic currents; t is time and has unit of ms; a, b, c and d are the parameters by tuning which various firing patterns can be generated; I represents synaptic currents or injected dc-currents to the neuron.

We choose to use this neuron model to simulate the voltage dynamics of individual neurons because: 1). It combines the biological plausibility of the Hodgkin–Huxley neuron model and the computational efficiency of leaky integrate-and-fire neuron model, allowing us to simulate tens of thousands of spiking neurons simultaneously in our network; 2). Different combinations of the parameter values a, b, c and d can reproduce a diversity of firing patterns of neurons of known types, so we can capture the biophysical diversity in the firing properties for different types of neurons in olfactory system, such as the mitral/tufted (M/T) cells and granule cells in the main olfactory bulb (MOB), and piriform cortical cells and other local inhibitory interneurons in piriform cortex (PCx). In order to achieve heterogeneity such that different cells within the same type exhibit different dynamics, we introduced randomness in the parameter assignment (see Table 1). The r_i is a random variable uniformly distributed on the interval [0,1] and i denotes the neuron index. For example, the parameter a will be distributed on the interval [0.02, 0.1] within which various firing patterns can emerge. We also used r_i^2 or r_i^4 to bias the distribution to different extent for different cell types. Overall, based on our choice of parameters in the Izhikevich model, the spiking patterns of PCs and M/T cells largely fall into the category of regular

spiking, intrinsically bursting or chattering neurons [21,94,95]. Inhibitory neurons including GCs and FFIs/FBIs in the network can generate spiking patterns as fast spiking neurons and low-threshold spiking neurons [96–99].

Synaptic input I to each neuron depends on the neuron type. For a cell i in MOB, I_i is a linear superposition of various sources

$$I_i = I_i^{mc-ex} + I_i^{gc-in} + I_i^{osn} + I_i^{feedback} + \xi_i \quad (3)$$

Here, I_i^{mc-ex} represents excitation from M/T cells and exists for both M/T cells and GCs. For GCs, when a M/T cells fires, the excitatory post-synaptic current (EPSC) I_i^{mc-ex} into different GCs are delayed by different latencies, resulting in different spiking latencies of GCs, consistent with previous experimental findings in the olfactory bulb granule cell network [56]. The I_i^{gc-in} represents inhibition from GCs and exists for both M/T cells and GCs. I_i^{osn} represents glomerular input and only exists for M/T cells. When a glomerulus is activated by a model odor, it provides correlated inputs I_i^{osn} to the M/T cells driven by that glomerulus. When a glomerulus is activated, the input current I_i^{osn} that an associated M/T cell receives is modelled as a step function with Gaussian noise added. Since each glomerulus receives inputs from a set of receptor neurons expressing the same olfactory gene type, the inputs to individual glomerulus from receptor neurons are substantially correlated [100–103]. Therefore, we assumed that the glomerular inputs to the apical dendrites received by the M/T cells associated with the same glomerulus were correlated. No input correlation between M/T cells associated with different glomeruli is assumed. I_i^{feedback} represents excitatory centrifugal input from piriform cells and is non-zero only for GCs when feedback is ON. We set it to zero for all GCs when feedback is OFF. The ξ_i represents Gaussian white noise input with zero mean and standard deviation σ = 1.75 for M/T cells and σ = 0.8 for GCs.

Similarly, for a cell i in PCx, I_i is composed of

$$I_i = I_i^{mob} + I_i^{pc-ex} + I_i^{in} + \eta_i \quad (4)$$

where I_i^{mob} represents input from M/T cells in MOB and only exists for piriform cortical cells (PCs) and feedforward inhibitory neurons (FFIs); I_i^{pc-ex} represents excitation from PCs and exists for both PCs and feedback inhibitory neurons (FBIs); I_i^{in} represents inhibition from local inhibitory neurons including FFIs and FBIs; η_i represents Gaussian white noise input (zero mean and standard deviation σ = 0.9) and only exists for PCs. Each action potential fired by a presynaptic neuron will evoke a jump in the corresponding synaptic inputs of all its postsynaptic targets by an amount equal to the appropriate synaptic strength. For example, action potentials of a M/T cell induce jumps in the excitatory currents of their postsynaptic target neurons, including I_i^{mc-ex} in M/T cells and GCs in MOB, and I_i^{mob} in FFIs and PCs in PCx. These synaptic inputs then decay to zero with time constant $10ms$. The height of the jump is determined by the pairwise synaptic strength between any two neurons and their values are given in the synaptic weight matrix which will described in the next section.

Synaptic strength and model network architecture

The MOB consists of 50 glomeruli, each of which drives 25 M/T cells, thus a total 1250 M/T cells in MOB. Besides, a local population of 12,500 inhibitory GCs formed reciprocal and lateral inhibitory connections with M/T cells. Thus, within the MOB, we have a weight matrix $\mathbf{W}_{mob}$ of 13,750 by 13,750 with its entry W_{mob}^{ij}representing the synaptic strength from presynaptic neuron j to postsynaptic neuron i. Depending on the cell type, this matrix $\mathbf{W}_{mob}$ can be partitioned into four sub-matrices, i.e., from M/T cell to M/T cell, from M/T cell to GC, from GC to M/T cell and from GC to GC. The specific value of each entry in $\mathbf{W}_{mob}$ was assigned randomly according to two parameters we chose for each sub-matrix. One is the connection density (the percentage of non-zero synaptic weights) and the other is the average synaptic strength (mean of a uniform distribution from

	M/T cells	GCs	PCs	FFIs/FBIs
a	$0.1-0.08r_i^4$	$0.1-0.08r_i^2$	$0.02+0.08r_i$	$0.1-0.08r_i^2$
b	0.2	0.2	0.2	0.2
c	-65	$-65+15r_i^2$	-65	$-65+15r_i^2$
d	$2+6r_i^4$	2	$8-6r_i$	2

Table 1. **Parameters of Izhikevich neuron model for different cell types**

which individual synaptic weights are sampled). Each sub-matrix has its own value of the connection density and average synaptic strength. In particular, the connection density and average synaptic strength between M/T cells driven by the same glomerulus are higher than between M/T cells driven by different glomeruli.

Individual M/T cell "projections" form random excitatory connections with 10,000 PCs and 1250 FFIs in PCx, giving rise to a feedforward weight matrix $\mathbf{W}_{ff}$ of 11,250 by 1250. Within PCx, PCs form recurrent excitations with each other. The FFIs inhibit both PCs and other FFIs, and another population of 1250 FBIs that receive input from a random subset of PCs inhibit PCs and other FBIs. Therefore, we have a matrix $\mathbf{W}_{pcx}$ of 12,500 by 12,500 that identifies all synaptic weights between cells in PCx. PCs "project" back to the MOB, providing excitatory centrifugal feedback to GCs, giving rise to a feedback weight matrix $\mathbf{W}_{fb}$ of 12,500 by 10,000. Under the condition of centrifugal feedback OFF, this $\mathbf{W}_{fb}$ is set to be a zero matrix. The connection density and average synaptic strength for all sub-matrices can be found in Table 2. The parameters are all chosen heuristically based on previous theoretical and experimental studies listed in Table 2.

Feedback projections from piriform cortex to the bulb may be structured, as retrograde rabies tracing demonstrates that piriform cells projecting to GC populations in the bulb tend to be spatially clustered [104]. Furthermore, a number of studies suggest that GC synapses are especially sensitive to plasticity [9,105], either through adult neurogenesis or more traditional mechanisms of synaptic reorganization. To implement all of these features, we structure the feedback projections to GCs such that the PCs receiving feedforward inputs from the M/T cells of certain glomeruli project back to the GCs which are reciprocally connected with M/T cells associated with other glomeruli. Reciprocal connectivity between M/T cells and GCs is defined as: M/T-1 excites GC-1 and GC-1 inhibits M/T-1, as observed by many studies [106,107]. Across the M/T population, there are 291 ± 9 (mean±SD, n = 1250 M/T cells) GCs that are reciprocally connected with each M/T cell. As a result, each PC projects to 7368 ± 64 GCs (mean±SD, n = 10000 PCs) with weight magnitude larger than 0.01. All feedback synaptic weights are randomly generated with small magnitude less than 0.05, and this structure gives rise to a dense but weak connectivity matrix $\mathbf{W}_{fb}$. Due to the sparsity of the PC firings when feedback is ON, this dense and weak top-down connectivity ensures robust influence of PCs on GC activity and thus the contribution of PCx on odor processing in MOB.

Model odor definition

Model odors are defined by the combinatorial patterns of glomeruli which are activated successively with different glomerular timing, a pattern recapitulating the spatiotemporal structure of odor inputs (Rubin and Katz, 1999; Meister and Bonhoeffer, 2001). Specifically, when a model odor is presented, 3~10 glomeruli will be activated (6 – 20% of all glomeruli) and all the M/T cells associated with those glomeruli will receive correlated glomerular input I^{osn}which lasts for 90ms. A table of 100 model odors were defined as the odor inputs to our network.

Modeling adult-neurogenesis as weight reshuffling

Adult-neurogenesis of the granule cells constantly removes old granule cells and replace them with adult-born ones. As a consequence, all the synapses from and onto old granule cells are removed and new synapses with adult-born ones are built. We modeled this process by weight reshuffling in the network with the total number of granule cells fixed. On each simulation day, 10% of the granule cells had their synaptic weights reshuffled. For each granule cell, the values of synaptic weights changed randomly on each day. The distributions from which new synaptic weights were sampled from were the same distributions as building the network (see Table 3.2). We only reshuffled the individual weight values without changing the whole weight distributions.

Principal component analysis (PCA)

Spiking activity of each mitral/tufted cell and each piriform cell was binned into a $5ms$ sliding time window and averaged across trials (each model odor was presented in 10 trials). To perform the PCA analysis, we concatenated the trial-averaged responses of all mitral/tufted cells to all 100 model odors on all simulation days, resulting in a large matrix of 1250 cells by 247 time bins × 100

	Connection density	Average synaptic strength	References
MCtoMC (same glomerulus)	0.8	0.25	2,108–110
MCtoMC (different glomeruli)*	0	0	
MC2GC	0.3	0.25	3,56,96,107
GC2MC	0.02	-0.4	
GC2GC	0.05	-0.1	63,96
MC2PC	0.5	0.06	4,6,22,111
MC2FFI	0.2	0.2	
PC2GC	0.9	0.03	64,112,113
PC2PC	0.01	0.1	22,72,99,114
FFI2PC	0.1	-0.1	
FBI2PC	0.8	-0.1	
FFI2FFI	0.01	-1.0	
PC2FBI	0.02	0.3	
FBI2FBI	0.02	-0.5	

*: We assumed zero connection between M/T cells associated with different glomeruli.

Table 2. **Network parameters controlling the connectivity between cell types.**

odors × 11 days. Response covariance matrices (1250 by 1250) were computed for this concatenated matrix (after subtracting the mean responses averaged across time bins, odors, and days). This gave us a single set of eigenvectors, thus the same eigenspace into which cell responses for all days can be projected and compared. Each 1250-dimensional cell response vector was then projected onto the first 3 principal eigenvectors for visualization and the first 50 principal eigenvectors for computations. The same procedure was also done for piriform cells. In our simulations, these PCs captured the majority of variance relevant for odor identity (~60–70% for M/T cells and ~55–65% for piriform cortex).

Population vectors of firing rates and PCA trajectories

We constructed the population vectors using either the firing rates of all cells or the PCA trajectories of the first 50 dimensions. When using the firing rates, for each odor on each day, the single-trial responses all the cells was a matrix of 1250 cells by 247 time bins for M/T cells or 10,000 cells by 247 time bins for piriform cells. We then converted the matrix into a long vector of lengths 1250 × 247 for M/T cells and 10,000 × 247 for piriform cells. When using PCA trajectories, the same procedures were applied, with only the cell number replaced by the reduced dimensionality.

Pairwise correlation between population vectors

To measure the similarity of population responses over time, we computed the Pearson's pairwise correlations of the population vectors constructed either by firing rates or PCA trajectories on two comparison days (for example, day-i and day-j). For within-odor correlation, the two population vectors were the responses (either single-trial or trial-averaged) to the same odor on day-i and day-j. For across-odor correlation, the two population vectors were the responses to any given two different odors on day-i and day-j, and we computed that for all different odor pairs on those two days. When $i = j$, the within-odor correlation was computed by comparing responses of even and odd trials.

Cosine similarity between population vectors

To gain a geometric perspective of the drift over days, we computed the cosine similarity of the population vectors by $\theta_{i,j} = \boldsymbol{u}_i \cdot \boldsymbol{u}_j / \|\boldsymbol{u}_i\| \times \|\boldsymbol{u}_j\|$, where $\theta_{i,j}$ is the cosine similarity between day-i and day-j, and $\boldsymbol{u}_i$ ($\boldsymbol{u}_j$) is the trial-averaged population vector on day-i (day-j). We also estimated the within-day variability for each odor on each day by computing the cosine similarity between the even trial-averaged and odd trial-averaged responses. For within-day cosine similarity when $i = j$, we subtracted the estimated within-day variability from the computed cosine similarity.

Decoding analysis: K nearest neighbor algorithm

The K nearest neighbor approach was used to decode odor identity from the projected ensemble responses of PCs to any given odor pair [54]. Consistent with the computation of symmetrized Kullback–Leibler divergence D_{KL}, analysis was performed in the space of the first 50 principal components. The original data was broken up into testing and training sets. The training sets established the location of PC responses to known odors (i.e., known PC responses) in the principal component space and the testing sets were probed with respect to these known PC responses. The Euclidian distance of the unknown odors to all PC responses was then calculated and the K nearest neighbors were used to determine to which odor the unknown PC activity was responding to. This process of generating testing and training sets was repeated 30 times, with each repeat reflecting a different random population of testing and training to ensure that the decoding accuracy was not a result of artifacts of selecting a single testing/training population. Free parameters in the K nearest neighbor algorithm include the ratio of testing to training data, and the number of nearest neighbors used in the calculation. For training/testing, we used ratios of 50%, 70% and 90%. We also examined the algorithm's accuracy when 3, 5 and 7 nearest neighbors were used.

Spike-timing-dependent plasticity (STDP)

To model the effect of spike trains on synaptic weights, we used the suppression model given in [51]. Each pre- and post-synaptic spike was assigned with an efficacy $\epsilon_i = 1 - e^{-(ti-ti-1)/\tau s}$, where ϵ_i is the efficacy of the ith spike, t_i and t_{i-1} are the timing of the ith and $(i-1)$th spike respectively, and τ_s is the suppression time constant. The effect of each pair of pre- and post-synaptic spikes on synaptic modification was given by $\Delta w_{ij} = \epsilon_i^{\text{pre}} \epsilon_j^{\text{pos}} F(\Delta t_{ij})$, where ϵ_i^p and ϵ_j^{pos} are the efficacies of the ith presynaptic spike and jth postsynaptic spike, respectively, and Δt_{ij} is the interval between the two spikes $t_j^{\text{pos}} - t_i^{\text{pre}}$. The function F represents the effect of temporal window for STDP, defined as:

$$F(\Delta t)\begin{cases} A_+ e^{-|\Delta t|/\tau_+} & \text{if} \quad \Delta t > 0 \\ A_- e^{-|\Delta t|/\tau_-} & \text{if} \quad \Delta t < 0 \end{cases} \tag{5}$$

Where A is the scaling factor, τ is the time constant, + means long-term potentiation (LTP) and − means long-term depression (LTD). We chose $\tau_s^{\text{pre}} = 34ms$, $\tau_S^{pos} = 75ms$. A and $\tau_{+/-}$ are drawn from normal distributions for each synapse, where $A_+ \sim \mathcal{N}(1.03,0.1)$, $A_- \sim \mathcal{N}(-0.51,0.01)$, $\tau_+ \sim \mathcal{N}(13.3, 1.7)$ (in ms), $\tau_- \sim \mathcal{N}(34.5, 1.6)$ (in ms), and $\mathcal{N}(\mu, \sigma)$ represents normal distribution with mean μ and standard deviation σ. In our model, STDP acts on two sets of connections. It applies to the synapses *onto* abGCs from M/T cells, GC/SAC cells, and PCx neurons. It also applies to the synapses *from* abGCs, including those onto M/T cells and GC/SAC cells.

Supplemental information

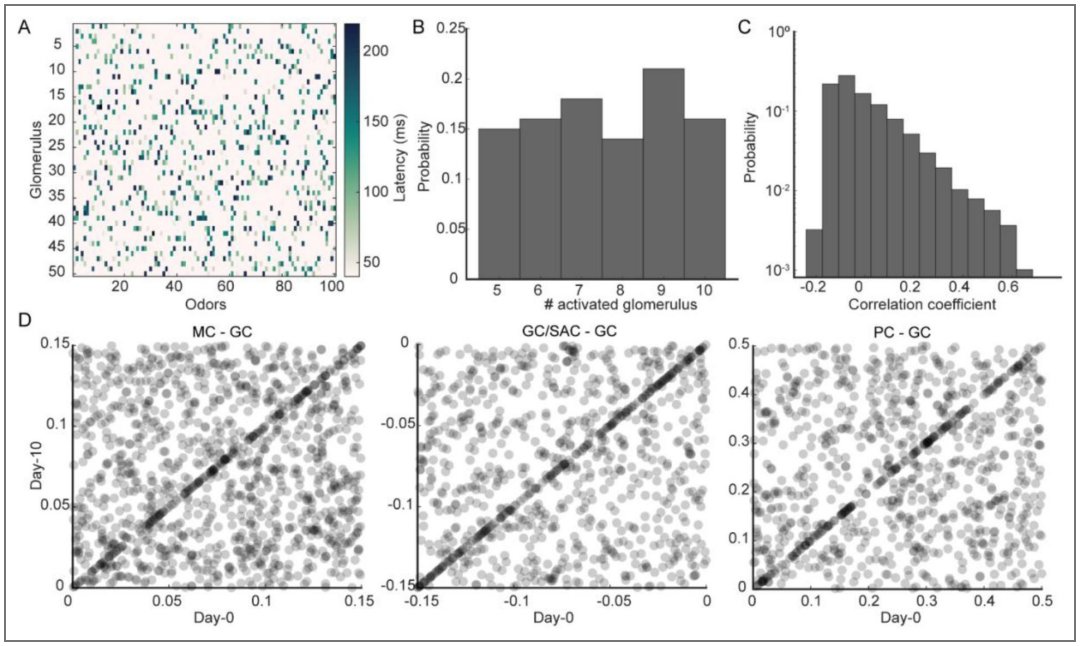

Fig. S1. Odor definition and synaptic weight changes (A). Glomerular activation latency for all 100 odors we defined. Each column corresponds to one odor. (B). Histogram of the number of activated glomeruli by all odors (n = 100 odors). (C). Histogram of correlation coefficients between each pair of odors, measuring the similarity between odors. (D). Sparsely sampled synaptic weights on day-0 (x axis) and day-10 (y axis). Each dot is a synapse. Left: M/T to GCs; middle: GC/SAC to GCs; right: PCs to GCs.

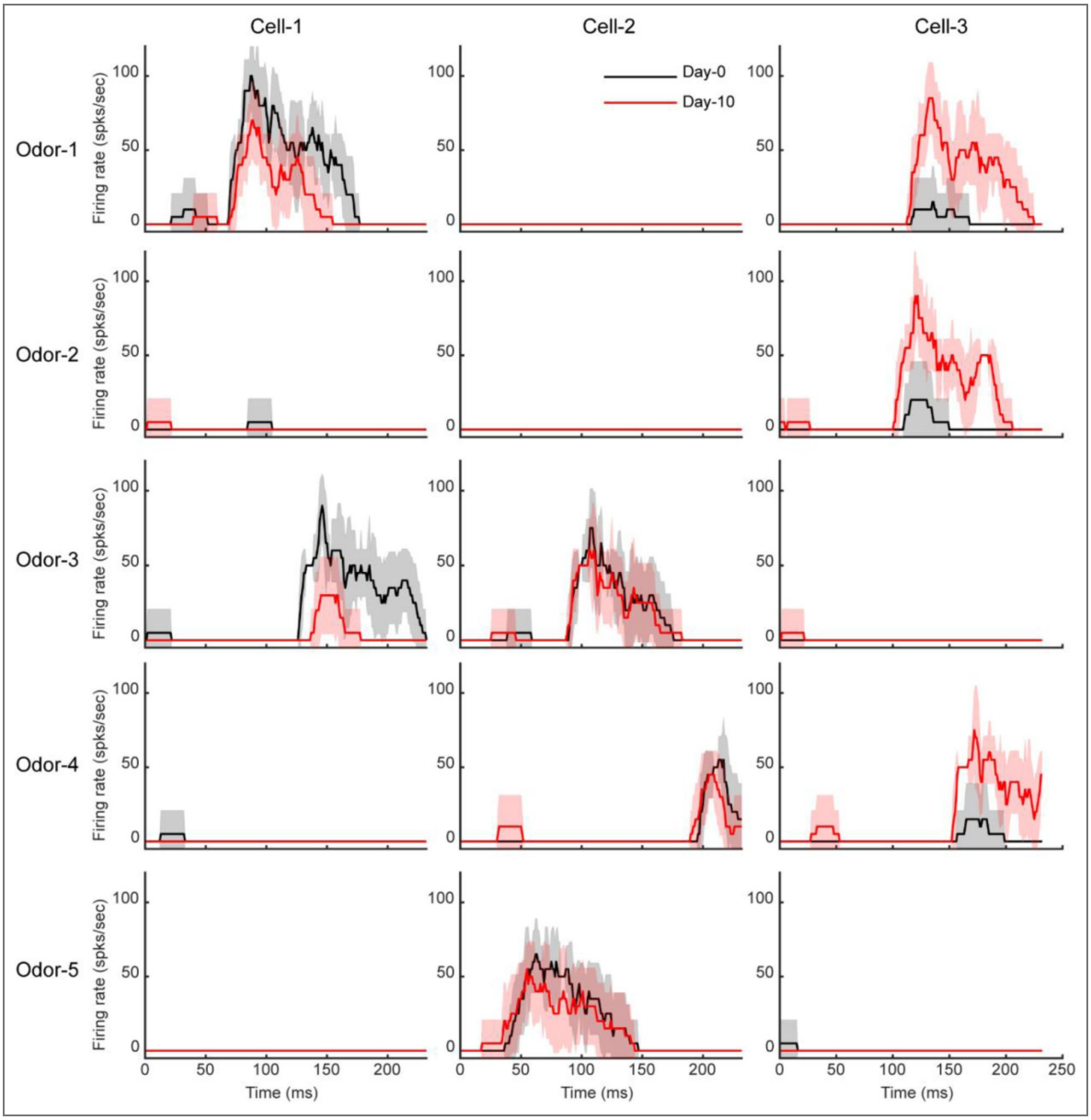

Fig. S2. Example M/T cell responses on day-0 and day-10

Three example M/T cells (column) in response to the five example odors (row). Black: response on day-0; red: response on day-10. Some cells increase their responses while some cells decrease their responses from day-0 to day-10 (mean ± SD, n = 10 trials).

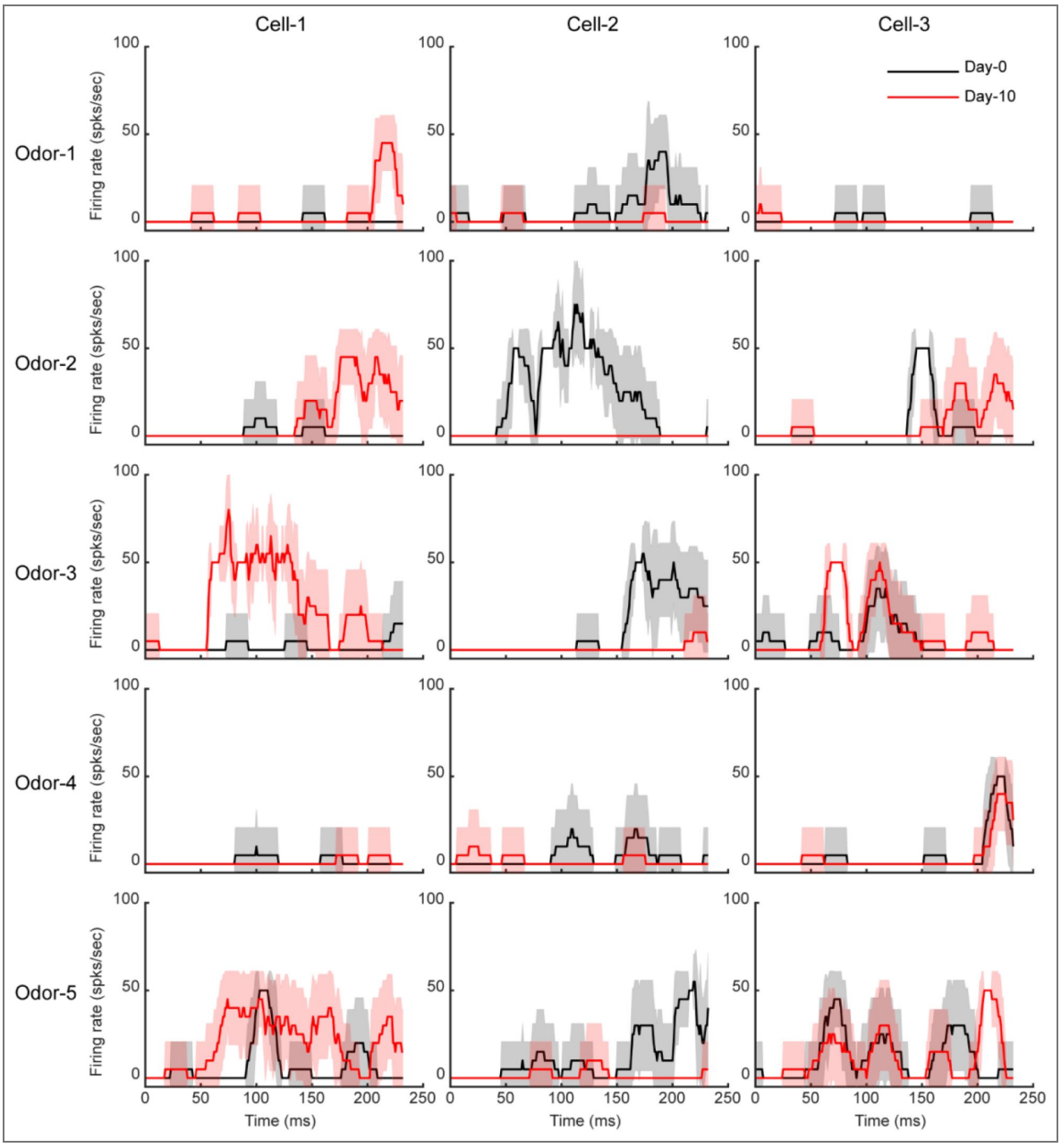

Fig. S3. Example Piriform cell responses on day-0 and day-10

Three example piriform cells (column) in response to the five example odors (row). Black: response on day-0; red: response on day-10 (mean ± SD, n = 10 trials).

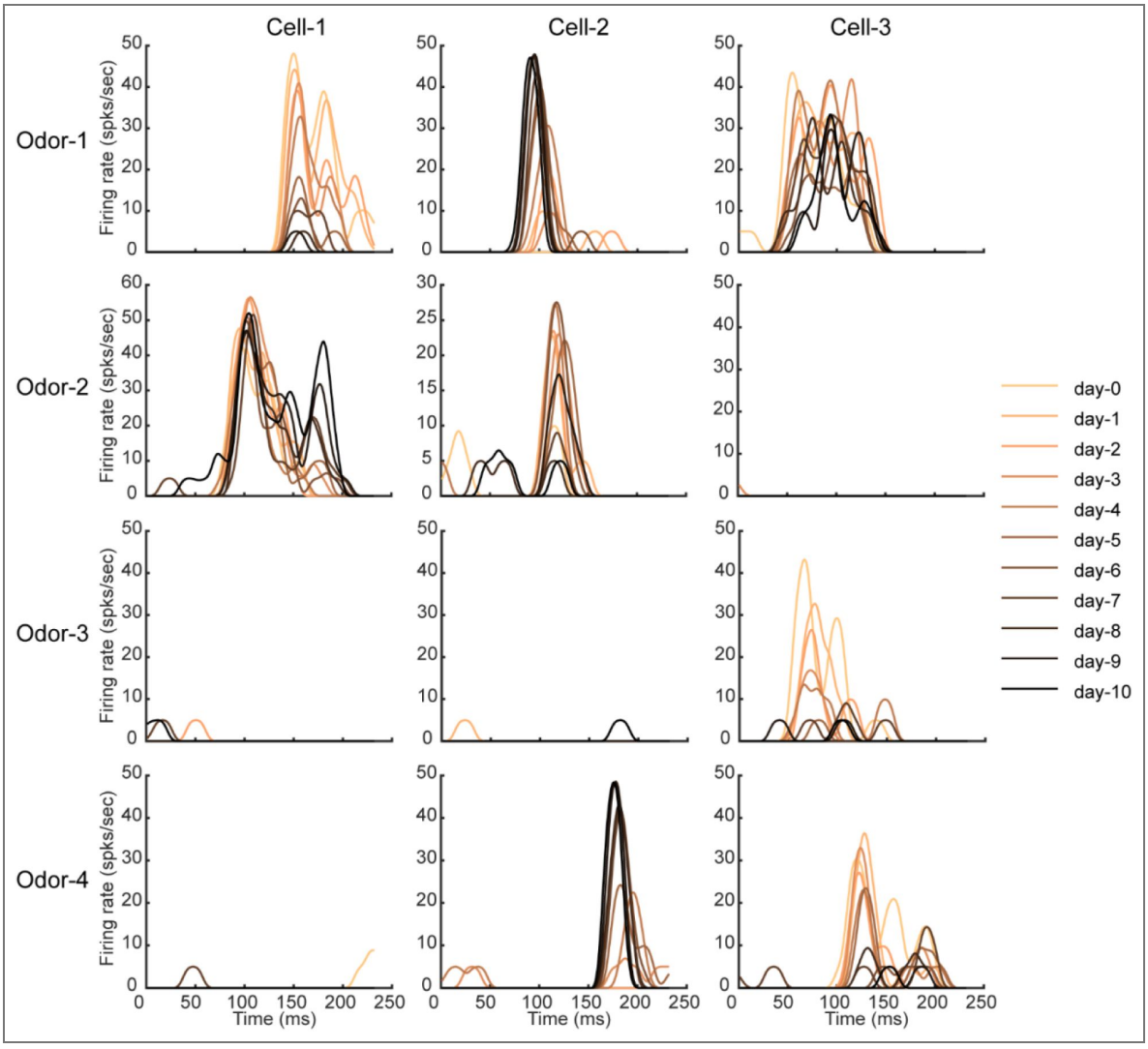

Fig. S4. Example piriform cell responses (trial-averaged) on all 10 days

(A). Another three example piriform cells in response to four odors from day-0 and day=10. Each curve is the response averaged across 10 trials (smoothed by a gaussian kernel with 20ms width). Note some piriform cells increase or decrease their responses, while some cells change their temporal profile (cell-3).

Fig. S5. Cell response changes between day-0 and day-10

(A). Histogram showing the differences between the trial-averaged response on day-10 and the trial-averaged response on day-0 for each odor-activated M/T cell (n=100 odors). Positive values indicate that the responses on day-10 are larger than day-0. (B). Same as (A) but for piriform cells.

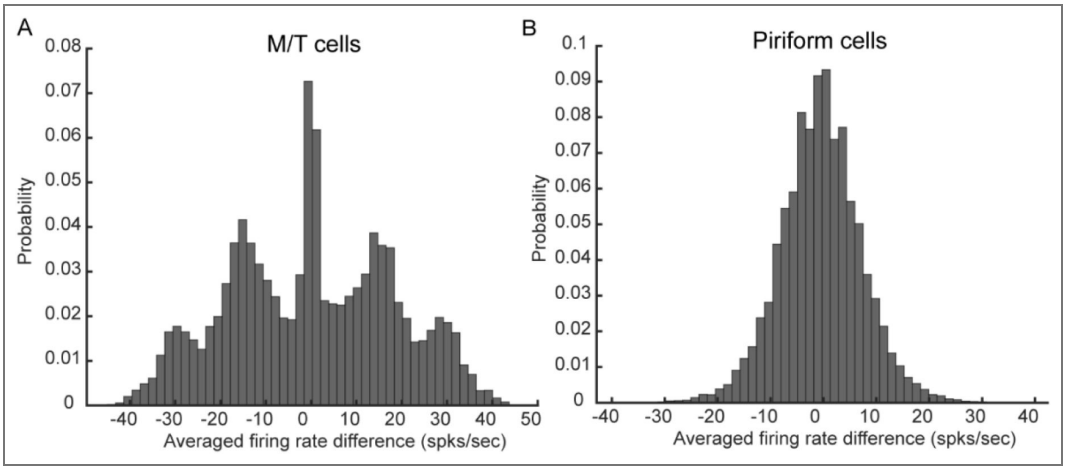

Fig. S6. Odor manifold and geometric reshaping of odor representations in PCx.

Odor manifolds of M/T cells (top) and PCs (bottom) on two example days (red and blue) are plotted by clusters of transparent round dots in the PCA space. Each column contains the trial-averaged trajectories on two days (red and blue) evoked by three example odors. M/T trajectories stay close while PCs trajectories are reshaped in different ways: shifted (A), rotated (B), and warped (C).

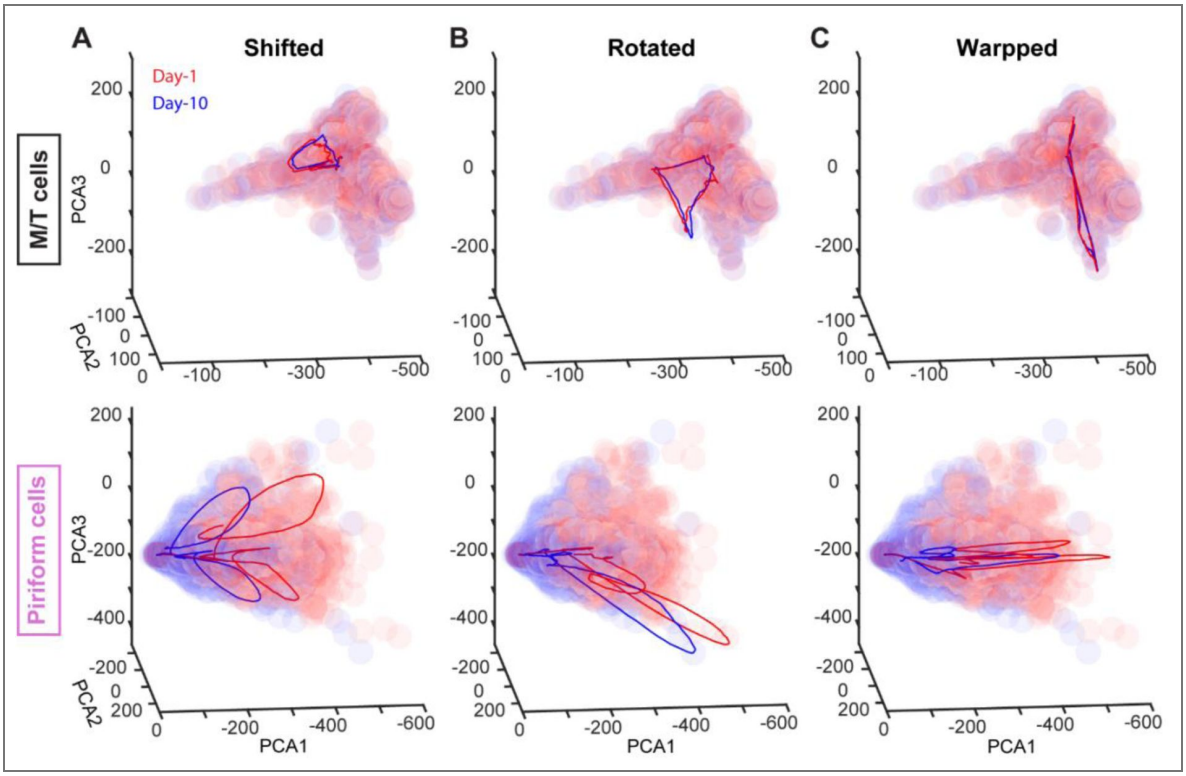

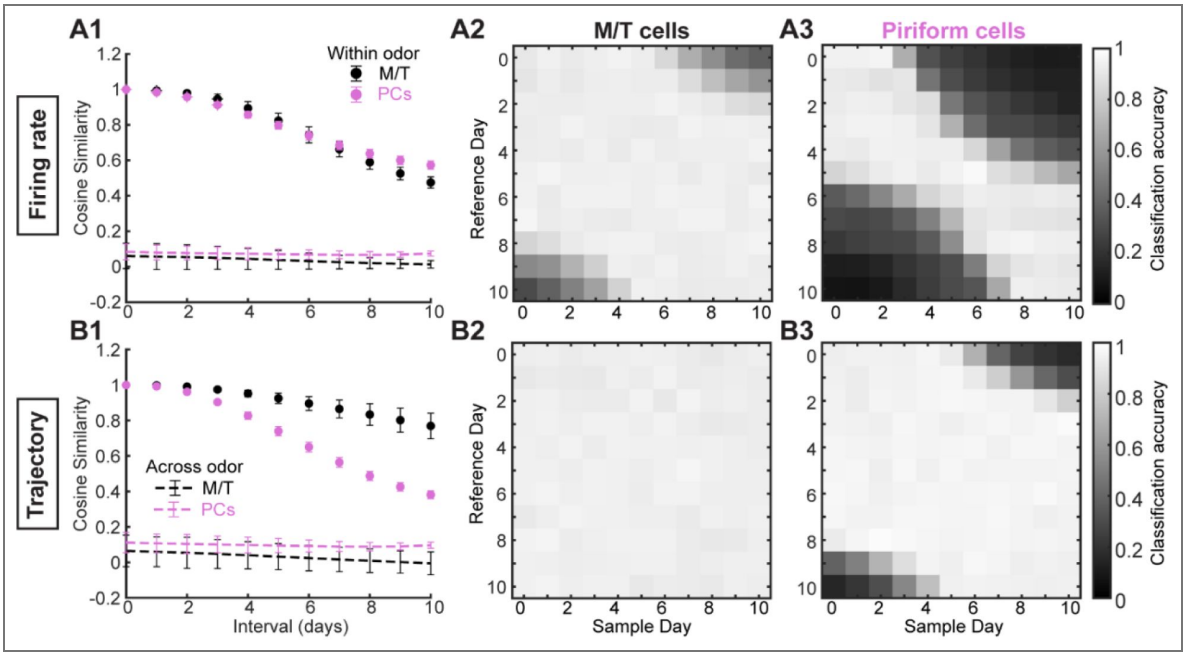

Fig. S7. Quantifying geometric reshaping and decoding analysis on M/T and PCs

(A1). Cosine similarity to quantify the geometric reshaping using population firing rate as a function of intervals (number of days separated). (A2). Decoding accuracy by K-nearest neighbors algorithm trained on M/T population firing rate of each sample day and tested on M/T population firing rate of each reference day. (A3). Same as (A2) but using PCs population firing rate. (B). Same as (A) but using PCA trajectories.

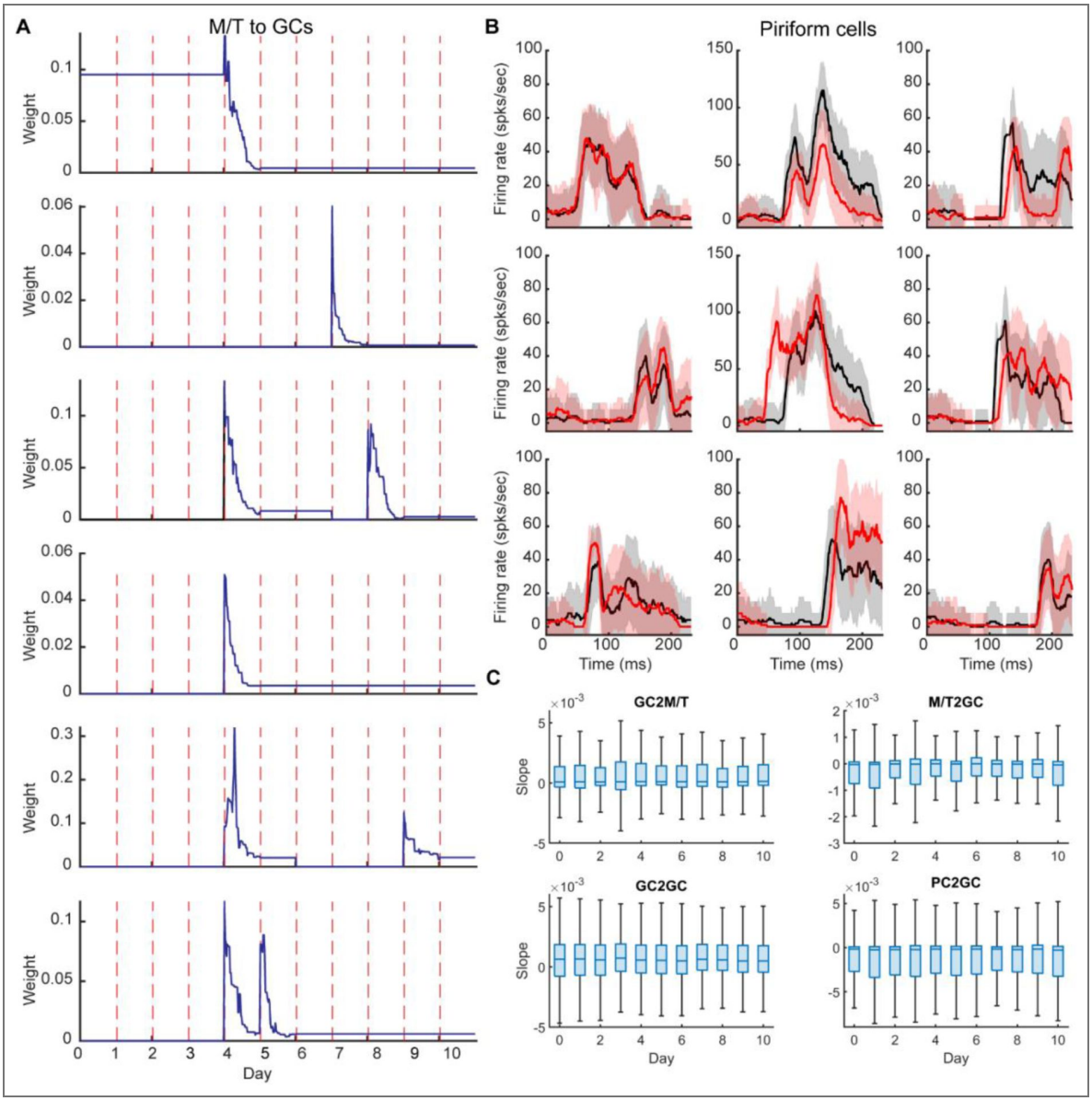

Fig. S8. Synaptic weight history of STDP

(A). Traces of five example synapses from M/T cells to GCs. STDP was applied when adult-neurogenesis happened at the start of the day. STDP drove the synaptic weight (y axis) to certain values through trial-by-trial exposure to certain odors. For some synapses, adult-neurogenesis only happened on one day while for other it happened on multiple days. (B). With STDP applied, three example piriform cells (column) in response to the three example odors (row). Black: response on day-0; red: response on day-10 (mean ± SD, n = 10 trials). (C). Slope of the synaptic weight traces over the last five trials of odor exposure with STPD applied. The slopes were all close to zero indicating the convergence of synaptic weights

Data availability

The current manuscript is a computational study, so no data have been generated for this manuscript. Modeling code is available via GitHub.

Acknowledgements

This study was supported by funding from the National Institutes of Health (NIH) and the National Science Foundation (NSF). KP was funded by NIH R01 MH113924, DC021141, NS135763, and NSF CAREER 1749772. This manuscript has been released as a pre-print.

Additional information

Author contributions

K.P. conceived and supervised the project. Z.C. performed the experiments and analyses. Z.C. and K.P. created the figures and wrote the manuscript. Both authors approved the submitted version.

Funding

Funder	Grant reference number	Author
HHS | NIH | National Institute of Neurological Disorders and Stroke (NINDS)	NS135763	Krishnan Padmanabhan
HHS | NIH | National Institute on Deafness and Other Communication Disorders (NIDCD)	DC021141	Krishnan Padmanabhan
HHS | NIH | National Institute of Mental Health (NIMH)	MH113924	Krishnan Padmanabhan
National Science Foundation (NSF)	1749772	Krishnan Padmanabhan

Author ORCID iDs

Zhen Chen: https://orcid.org/0000-0002-5590-3552
Krishnan Padmanabhan: https://orcid.org/0000-0002-3255-8346

References

1. **Lledo P.-M.,** Alonso M., Grubb M. S. (2006) Adult neurogenesis and functional plasticity in neuronal circuits. *Nat Rev Neurosci* **7**:179-193 https://doi.org/10.1038/nrn1867 | PubMed
2. **Urban N. N.,** Sakmann B. (2002) Reciprocal intraglomerular excitation and intra- and interglomerular lateral inhibition between mouse olfactory bulb mitral cells. *The Journal of Physiology* **542**:355-367 https://doi.org/10.1113/jphysiol.2001.013491 | PubMed
3. **Schoppa N. E.,** Urban N. N. (2003) Dendritic processing within olfactory bulb circuits. *Trends in Neurosciences* **26**:501-506 https://doi.org/10.1016/s0166-2236(03)00228-5 | PubMed
4. **Sosulski D. L.,** Bloom M. L., Cutforth T., Axel R., Datta S. R. (2011) Distinct representations of olfactory information in different cortical centres. *Nature* **472**:213-216 https://doi.org/10.1038/nature09868 | PubMed
5. **Ghosh S.,** et al. (2011) Sensory maps in the olfactory cortex defined by long-range viral tracing of single neurons. *Nature* **472**:217-220 https://doi.org/10.1038/nature09945 | PubMed
6. **Miyamichi K.,** et al. (2011) Cortical representations of olfactory input by trans-synaptic tracing. *Nature* **472**:191-196 https://doi.org/10.1038/nature09714 | PubMed

7. **Lepousez G.,** Valley M. T., Lledo P.-M. (2013) The Impact of Adult Neurogenesis on Olfactory Bulb Circuits and Computations. *Annu. Rev. Physiol* **75**:339-363 https://doi.org/10.1146/annurev-physiol-030212-183731 | PubMed
8. **Lepousez G.,** et al. (2014) Olfactory learning promotes input-specific synaptic plasticity in adult-born neurons. *Proceedings of the National Academy of Sciences* **111**:13984-13989 https://doi.org/10.1073/pnas.1404991111 | PubMed
9. **Livneh Y.,** Mizrahi A. (2012) Experience-dependent plasticity of mature adult-born neurons. *Nat Neurosci* **15**:26-28 https://doi.org/10.1038/nn.2980 | PubMed
10. **Nissant A.,** Bardy C., Katagiri H., Murray K., Lledo P.-M. (2009) Adult neurogenesis promotes synaptic plasticity in the olfactory bulb. *Nat Neurosci* **12**:728-730 https://doi.org/10.1038/nn.2298 | PubMed
11. **Lledo P.-M.,** Valley M. (2016) Adult Olfactory Bulb Neurogenesis. *Cold Spring Harb Perspect Biol* **8**:a018945 https://doi.org/10.1101/cshperspect.a018945 | PubMed
12. **Breton-Provencher V.,** Lemasson M., Peralta M. R., Saghatelyan A. (2009) Interneurons produced in adulthood are required for the normal functioning of the olfactory bulb network and for the execution of selected olfactory behaviors. *Journal of Neuroscience* **29**:15245-15257 https://doi.org/10.1523/jneurosci.3606-09.2009 | PubMed
13. **Kouremenou I.,** Piper M., Zalucki O. (2020) Adult Neurogenesis in the Olfactory System: Improving Performance for Difficult Discrimination Tasks?. *BioEssays* **42**:2000065 https://doi.org/10.1002/bies.202000065 | PubMed
14. **Bekkers J. M.,** Suzuki N. (2013) Neurons and circuits for odor processing in the piriform cortex. *Trends in Neurosciences* **36**:429-438 https://doi.org/10.1016/j.tins.2013.04.005 | PubMed
15. **Choi G. B.,** et al. (2011) Driving Opposing Behaviors with Ensembles of Piriform Neurons. *Cell* **146**:1004-1015 https://doi.org/10.1016/j.cell.2011.07.041 | PubMed
16. **Smear M.,** Resulaj A., Zhang J., Bozza T., Rinberg D. (2013) Multiple perceptible signals from a single olfactory glomerulus. *Nat Neurosci* **16**:1687-1691 https://doi.org/10.1038/nn.3519 | PubMed
17. **Chong E.,** et al. (2020) Manipulating synthetic optogenetic odors reveals the coding logic of olfactory perception. *Science* **368**:eaba2357 https://doi.org/10.1126/science.aba2357 | PubMed
18. **Gill J. V.,** et al. (2020) Precise Holographic Manipulation of Olfactory Circuits Reveals Coding Features Determining Perceptual Detection. *Neuron* **108**:382-393.e5 https://doi.org/10.1016/j.neuron.2020.07.034 | PubMed
19. **Mombaerts P.,** et al. (1996) Visualizing an Olfactory Sensory Map. *Cell* **87**:675-686 https://doi.org/10.1016/s0092-8674(00)81387-2 | PubMed
20. **Buck L.,** Axel R. (1991) A novel multigene family may encode odorant receptors: a molecular basis for odor recognition. *Cell* **65**:175-187 https://doi.org/10.1016/0092-8674(91)90418-x | PubMed
21. **Davison I. G.,** Ehlers M. D. (2011) Neural Circuit Mechanisms for Pattern Detection and Feature Combination in Olfactory Cortex. *Neuron* **70**:82-94 https://doi.org/10.1016/j.neuron.2011.02.047 | PubMed
22. **Stern M.,** Bolding K. A., Abbott L., Franks K. M. (2018) A transformation from temporal to ensemble coding in a model of piriform cortex. *eLife* **7**:e34831 https://doi.org/10.7554/eLife.34831 | PubMed
23. **Pashkovski S. L.,** et al. (2020) Structure and flexibility in cortical representations of odour space. *Nature* **583**:253-258 https://doi.org/10.1038/s41586-020-2451-1 | PubMed
24. **Schoonover C. E.,** Ohashi S. N., Axel R., Fink A. J. P. (2021) Representational drift in primary olfactory cortex. *Nature* **594**:541-546 https://doi.org/10.1038/s41586-021-03628-7 | PubMed
25. **Kanter E. D.,** Haberly L. B. (1990) NMDA-dependent induction of long-term potentiation in afferent and association fiber systems of piriform cortex in vitro. *Brain research* **525**:175-179 https://doi.org/10.1016/0006-8993(90)91337-g | PubMed
26. **Jung M. W.,** Larson J. (1994) Further characteristics of long-term potentiation in piriform cortex. *Synapse* **18**:298-306 https://doi.org/10.1002/syn.890180405 | PubMed

27. **Ziv Y.,** et al. (2013) Long-term dynamics of CA1 hippocampal place codes. *Nature neuroscience* **16**:264-266 https://doi.org/10.1038/nn.3329 | PubMed

28. **Haberly L. B.,** Bower J. M. (1984) Analysis of association fiber system in piriform cortex with intracellular recording and staining techniques. *Journal of Neurophysiology* **51**:90-112 https://doi.org/10.1152/jn.1984.51.1.90 | PubMed

29. **Haberly L. B.** (2001) Parallel-distributed Processing in Olfactory Cortex: New Insights from Morphological and Physiological Analysis of Neuronal Circuitry. *Chem Senses* **26**:551-576 https://doi.org/10.1093/chemse/26.5.551 | PubMed

30. **Aimone J. B.,** Gage F. H. (2011) Modeling new neuron function: a history of using computational neuroscience to study adult neurogenesis. *European Journal of Neuroscience* **33**:1160-1169 https://doi.org/10.1111/j.1460-9568.2011.07615.x | PubMed

31. **Pignatelli A.,** Belluzzi O. (2010) Neurogenesis in the Adult Olfactory Bulb. In: Menini A. (Ed). *The Neurobiology of Olfaction* Boca Raton (FL): CRC Press/Taylor & Francis. PubMed

32. **Fantana A. L.,** Soucy E. R., Meister M. (2008) Rat Olfactory Bulb Mitral Cells Receive Sparse Glomerular Inputs. *Neuron* **59**:802-814 https://doi.org/10.1016/j.neuron.2008.07.039 | PubMed

33. **Gschwend O.,** Beroud J., Vincis R., Rodriguez I., Carleton A. (2016) Dense encoding of natural odorants by ensembles of sparsely activated neurons in the olfactory bulb. *Sci Rep* **6**:36514 https://doi.org/10.1038/srep36514 | PubMed

34. **Vincis R.,** Gschwend O., Bhaukaurally K., Beroud J., Carleton A. (2012) Dense representation of natural odorants in the mouse olfactory bulb. *Nat Neurosci* **15**:537-539 https://doi.org/10.1038/nn.3057 | PubMed

35. **Rinberg D.,** Koulakov A., Gelperin A. (2006) Speed-Accuracy Tradeoff in Olfaction. *Neuron* **51**:351-358 https://doi.org/10.1016/j.neuron.2006.07.013 | PubMed

36. **Uchida N.,** Mainen Z. F. (2003) Speed and accuracy of olfactory discrimination in the rat. *Nat Neurosci* **6**:1224-1229 https://doi.org/10.1038/nn1142 | PubMed

37. **Wesson D. W.,** Carey R. M., Verhagen J. V., Wachowiak M. (2008) Rapid Encoding and Perception of Novel Odors in the Rat. *PLoS Biol* **6**:e82 https://doi.org/10.1371/journal.pbio.0060082 | PubMed

38. **Kato H. K.,** Chu M. W., Isaacson J. S., Komiyama T. (2012) Dynamic Sensory Representations in the Olfactory Bulb: Modulation by Wakefulness and Experience. *Neuron* **76**:962-975 https://doi.org/10.1016/j.neuron.2012.09.037 | PubMed

39. **Uchida N.,** Poo C., Haddad R. (2014) Coding and Transformations in the Olfactory System. *Annu. Rev. Neurosci* **37**:363-385 https://doi.org/10.1146/annurev-neuro-071013-013941 | PubMed

40. **Yamada Y.,** et al. (2017) Context- and Output Layer-Dependent Long-Term Ensemble Plasticity in a Sensory Circuit. *Neuron* **93**:1198-1212.e5 https://doi.org/10.1016/j.neuron.2017.02.006 | PubMed

41. **Shani-Narkiss H.,** Beniaguev D., Segev I., Mizrahi A. (2023) Stability and flexibility of odor representations in the mouse olfactory bulb. *Front. Neural Circuits* **17** https://doi.org/10.3389/fncir.2023.1157259 | PubMed

42. **Langdon C.,** Genkin M., Engel T. A. (2023) A unifying perspective on neural manifolds and circuits for cognition. *Nat Rev Neurosci* 1-15 https://doi.org/10.1038/s41583-023-00693-x | PubMed

43. **Kriegeskorte N.,** Wei X.-X. (2021) Neural tuning and representational geometry. *Nat Rev Neurosci* **22**:703-718 https://doi.org/10.1038/s41583-021-00502-3 | PubMed

44. **Baker K. L.,** Vasan G., Gumaste A., Pieribone V. A., Verhagen J. V. (2019) Spatiotemporal dynamics of odor responses in the lateral and dorsal olfactory bulb. *PLoS Biol* **17**:e3000409 https://doi.org/10.1371/journal.pbio.3000409 | PubMed

45. **Gire D. H.,** et al. (2013) Temporal Processing in the Olfactory System: Can We See a Smell?. *Neuron* **78**:416-432 https://doi.org/10.1016/j.neuron.2013.04.033 | PubMed

46. **Schaefer A. T.,** Margrie T. W. (2007) Spatiotemporal representations in the olfactory system. *Trends in Neurosciences* **30**:92-100 https://doi.org/10.1016/j.tins.2007.01.001 | PubMed

47. **Rennaker R. L.,** Chen C.-F. F., Ruyle A. M., Sloan A. M., Wilson D. A. (2007) Spatial and Temporal Distribution of Odorant-Evoked Activity in the Piriform Cortex. *Journal of Neuroscience* **27**:1534-1542 https://doi.org/10.1523/jneurosci.4072-06.2007 | PubMed

48. **Chen Z.,** Padmanabhan K. (2022) Top-down feedback enables flexible coding strategies in the olfactory cortex. *Cell Reports* **38**:110545 https://doi.org/10.1016/j.celrep.2022.110545 | PubMed

49. **Haddad R.,** et al. (2013) Olfactory cortical neurons read out a relative time code in the olfactory bulb. *Nat Neurosci* **16**:949-957 https://doi.org/10.1038/nn.3407 | PubMed

50. **Wu A.,** et al. (2020) Context-dependent plasticity of adult-born neurons regulated by cortical feedback. *Sci. Adv* **6**:eabc8319 https://doi.org/10.1126/sciadv.abc8319 | PubMed

51. **Froemke R. C.,** Dan Y. (2002) Spike-timing-dependent synaptic modification induced by natural spike trains. *Nature* **416**:433-438 https://doi.org/10.1038/416433a | PubMed

52. **Bi G.,** Poo M. (2001) Synaptic Modification by Correlated Activity: Hebb's Postulate Revisited. *Annual Review of Neuroscience* **24**:139-166 https://doi.org/10.1146/annurev.neuro.24.1.139 | PubMed

53. **Markram H.,** Gerstner W., Sjöström P. J. (2012) Spike-Timing-Dependent Plasticity: A Comprehensive Overview. *Front. Synaptic Neurosci* **4** https://doi.org/10.3389/fnsyn.2012.00002 | PubMed

54. **Padmanabhan K.,** Urban N. N. (2010) Intrinsic biophysical diversity decorrelates neuronal firing while increasing information content. *Nat Neurosci* **13**:1276-1282 https://doi.org/10.1038/nn.2630 | PubMed

55. **Angelo K.,** Margrie T. W. (2011) Population diversity and function of hyperpolarization-activated current in olfactory bulb mitral cells. *Sci Rep* **1**:50 https://doi.org/10.1038/srep00050 | PubMed

56. **Kapoor V.,** Urban N. N. (2006) Glomerulus-Specific, Long-Latency Activity in the Olfactory Bulb Granule Cell Network. *Journal of Neuroscience* **26**:11709-11719 https://doi.org/10.1523/jneurosci.3371-06.2006 | PubMed

57. **Friedrich R. W.,** Laurent G. (2001) Dynamic Optimization of Odor Representations by Slow Temporal Patterning of Mitral Cell Activity. *Science* **291**:889-894 https://doi.org/10.1126/science.291.5505.889 | PubMed

58. **Smear M.,** Shusterman R., O'Connor R., Bozza T., Rinberg D. (2011) Perception of sniff phase in mouse olfaction. *Nature* **479**:397-400 https://doi.org/10.1038/nature10521 | PubMed

59. **Laurent G.** (2002) Olfactory network dynamics and the coding of multidimensional signals. *Nature reviews neuroscience* **3**:884-895 https://doi.org/10.1038/nrn964 | PubMed

60. **Schreck M. R.,** et al. (2022) State-dependent olfactory processing in freely behaving mice. *Cell Reports* **38** https://doi.org/10.1016/j.celrep.2022.110450 | PubMed

61. **Chockanathan U.,** et al. (2021) Changes in pairwise correlations during running reshape global network state in the main olfactory bulb. *Journal of neurophysiology* **125**:1612-1623 https://doi.org/10.1152/jn.00464.2020 | PubMed

62. **D'Souza R. D.,** Vijayaraghavan S. (2014) Paying attention to smell: cholinergic signaling in the olfactory bulb. *Front. Synaptic Neurosci* **6** https://doi.org/10.3389/fnsyn.2014.00021 | PubMed

63. **Boyd A. M.,** Sturgill J. F., Poo C., Isaacson J. S. (2012) Cortical Feedback Control of Olfactory Bulb Circuits. *Neuron* **76**:1161-1174 https://doi.org/10.1016/j.neuron.2012.10.020 | PubMed

64. **Otazu G. H.,** Chae H., Davis M. B., Albeanu D. F. (2015) Cortical Feedback Decorrelates Olfactory Bulb Output in Awake Mice. *Neuron* **86**:1461-1477 https://doi.org/10.1016/j.neuron.2015.05.023 | PubMed

65. **Magavi S. S. P.,** Mitchell B. D., Szentirmai O., Carter B. S., Macklis J. D. (2005) Adult-Born and Preexisting Olfactory Granule Neurons Undergo Distinct Experience-Dependent Modifications of their Olfactory Responses In Vivo. *J. Neurosci* **25**:10729-10739 https://doi.org/10.1523/jneurosci.2250-05.2005 | PubMed

66. **Kaplan M. S.,** McNelly N. A., Hinds J. W. (1985) Population dynamics of adult-formed granule neurons of the rat olfactory bulb. *Journal of Comparative Neurology* **239**:117-125 https://doi.org/10.1002/cne.902390110 | PubMed

67. **Petreanu L.,** Alvarez-Buylla A. (2002) Maturation and Death of Adult-Born Olfactory Bulb Granule Neurons: Role of Olfaction. *J. Neurosci* **22**:6106-6113 https://doi.org/10.1523/JNEUROSCI.22-14-06106.2002 | PubMed

68. **Kamimura S.,** et al. (2022) New granule cells in the olfactory bulb are associated with high respiratory input in an enriched odor environment. *Neuroscience Research* **182**:52-59 https://doi.org/10.1016/j.neures.2022.05.007 | PubMed

69. **van Praag H.,** Christie B. R., Sejnowski T. J., Gage F. H. (1999) Running enhances neurogenesis, learning, and long-term potentiation in mice. *Proceedings of the National Academy of Sciences* **96**:13427-13431 https://doi.org/10.1073/pnas.96.23.13427 | PubMed

70. **Gheusi G.,** Lledo P.-M. (2014) Adult Neurogenesis in the Olfactory System Shapes Odor Memory and Perception. *Progress in Brain Research* **208**:157-175 https://doi.org/10.1016/b978-0-444-63350-7.00006-1 | PubMed

71. **Alonso M.,** et al. (2006) Olfactory Discrimination Learning Increases the Survival of Adult-Born Neurons in the Olfactory Bulb. *Journal of Neuroscience* **26**:10508-10513 https://doi.org/10.1523/jneurosci.2633-06.2006 | PubMed

72. **Franks K. M.,** et al. (2011) Recurrent Circuitry Dynamically Shapes the Activation of Piriform Cortex. *Neuron* **72**:49-56 https://doi.org/10.1016/j.neuron.2011.08.020 | PubMed

73. **Apicella A.,** Yuan Q., Scanziani M., Isaacson J. S. (2010) Pyramidal Cells in Piriform Cortex Receive Convergent Input from Distinct Olfactory Bulb Glomeruli. *Journal of Neuroscience* **30**:14255-14260 https://doi.org/10.1523/jneurosci.2747-10.2010 | PubMed

74. **Blazing R. M.,** Franks K. M. (2020) Odor coding in piriform cortex: mechanistic insights into distributed coding. *Current Opinion in Neurobiology* **64**:96-102 https://doi.org/10.1016/j.conb.2020.03.001 | PubMed

75. **Chae H.,** Banerjee A., Dussauze M., Albeanu D. F. (2022) Long-range functional loops in the mouse olfactory system and their roles in computing odor identity. *Neuron* S0896627322008108 https://doi.org/10.1016/j.neuron.2022.09.005 | PubMed

76. **Zeppilli S.,** et al. (2021) Molecular characterization of projection neuron subtypes in the mouse olfactory bulb. *eLife* **10**:e65445 https://doi.org/10.7554/eLife.65445 | PubMed

77. **Fink A. J. P.,** et al. (2025) Experience-dependent reorganization of inhibitory neuron synaptic connectivity. *bioRxiv* https://doi.org/10.1101/2025.01.16.633450

78. **Lemasson M.,** Saghatelyan A., Olivo-Marin J.-C., Lledo P.-M. (2005) Neonatal and adult neurogenesis provide two distinct populations of newborn neurons to the mouse olfactory bulb. *Journal of Neuroscience* **25**:6816-6825 https://doi.org/10.1523/jneurosci.1114-05.2005 | PubMed

79. **Whitman M. C.,** Greer C. A. (2009) Adult neurogenesis and the olfactory system. *Progress in Neurobiology* **89**:162-175 https://doi.org/10.1016/j.pneurobio.2009.07.003 | PubMed

80. **Qin S.,** et al. (2023) Coordinated drift of receptive fields in Hebbian/anti-Hebbian network models during noisy representation learning. *Nat Neurosci* **26**:339-349 https://doi.org/10.1038/s41593-022-01225-z | PubMed

81. **Driscoll L. N.,** Pettit N. L., Minderer M., Chettih S. N., Harvey C. D. (2017) Dynamic reorganization of neuronal activity patterns in parietal cortex. *Cell* **170**:986-999 https://doi.org/10.1016/j.cell.2017.07.021 | PubMed

82. **Rokni U.,** Richardson A. G., Bizzi E., Seung H. S. (2007) Motor learning with unstable neural representations. *Neuron* **54**:653-666 https://doi.org/10.1016/j.neuron.2007.04.030 | PubMed

83. **Lee J. S.,** Briguglio J. J., Cohen J. D., Romani S., Lee A. K. (2020) The statistical structure of the hippocampal code for space as a function of time, context, and value. *Cell* **183**:620-635 https://doi.org/10.1016/j.cell.2020.09.024 | PubMed

84. **Gonzalez W. G.,** Zhang H., Harutyunyan A., Lois C. (2019) Persistence of neuronal representations through time and damage in the hippocampus. *Science* **365**:821-825 https://doi.org/10.1126/science.aav9199 | PubMed

85. **Toda T.,** Parylak S. L., Linker S. B., Gage F. H. (2019) The role of adult hippocampal neurogenesis in brain health and disease. *Mol Psychiatry* **24**:67-87 https://doi.org/10.1038/s41380-018-0036-2 | PubMed

86. **Hainmueller T.,** Bartos M. (2018) Parallel emergence of stable and dynamic memory engrams in the hippocampus. *Nature* **558**:292-296 https://doi.org/10.1038/s41586-018-0191-2 | PubMed

87. **Lazarini F.,** Lledo P.-M. (2011) Is adult neurogenesis essential for olfaction?. *Trends in Neurosciences* **34**:20-30 https://doi.org/10.1016/j.tins.2010.09.006 | PubMed

88. **Gheusi G.,** et al. (2000) Importance of newly generated neurons in the adult olfactory bulb for odor discrimination. *Proceedings of the National Academy of Sciences* **97**:1823-1828 https://doi.org/10.1073/pnas.97.4.1823 | PubMed

89. **Brann J. H.,** Firestein S. J. (2014) A lifetime of neurogenesis in the olfactory system. *Front. Neurosci* **8** https://doi.org/10.3389/fnins.2014.00182 | PubMed

90. **Gonçalves J. T.,** Schafer S. T., Gage F. H. (2016) Adult Neurogenesis in the Hippocampus: From Stem Cells to Behavior. *Cell* **167**:897-914 https://doi.org/10.1016/j.cell.2016.10.021 | PubMed

91. **Jurkowski M. P.,** et al. (2020) Beyond the Hippocampus and the SVZ: Adult Neurogenesis Throughout the Brain. *Frontiers in Cellular Neuroscience* **14** https://doi.org/10.3389/fncel.2020.576444 | PubMed

92. **Sailor K. A.,** Schinder A. F., Lledo P.-M. (2017) Adult neurogenesis beyond the niche: its potential for driving brain plasticity. *Current Opinion in Neurobiology* **42**:111-117 https://doi.org/10.1016/j.conb.2016.12.001 | PubMed

93. **Izhikevich E. M.** (2003) Simple model of spiking neurons. *IEEE Trans. Neural Netw* **14**:1569-1572 https://doi.org/10.1109/tnn.2003.820440 | PubMed

94. **Connors B. W.,** Gutnick M. J. (1990) Intrinsic firing patterns of diverse neocortical neurons. *Trends in Neurosciences* **13**:99-104 https://doi.org/10.1016/0166-2236(90)90185-d | PubMed

95. **Padmanabhan K.,** Urban N. N. (2014) Disrupting information coding via block of 4-AP-sensitive potassium channels. *Journal of Neurophysiology* **112**:1054-1066 https://doi.org/10.1152/jn.00823.2013 | PubMed

96. **Burton S. D.,** Urban N. N. (2015) Rapid Feedforward Inhibition and Asynchronous Excitation Regulate Granule Cell Activity in the Mammalian Main Olfactory Bulb. *Journal of Neuroscience* **35**:14103-14122 https://doi.org/10.1523/jneurosci.0746-15.2015 | PubMed

97. **Egger V.,** Svoboda K., Mainen Z. F. (2005) Dendrodendritic Synaptic Signals in Olfactory Bulb Granule Cells: Local Spine Boost and Global Low-Threshold Spike. *Journal of Neuroscience* **25**:3521-3530 https://doi.org/10.1523/jneurosci.4746-04.2005 | PubMed

98. **Gibson J. R.,** Beierlein M., Connors B. W. (1999) Two networks of electrically coupled inhibitory neurons in neocortex. *Nature* **402**:75-79 https://doi.org/10.1038/47035 | PubMed

99. **Suzuki N.,** Bekkers J. M. (2012) Microcircuits Mediating Feedforward and Feedback Synaptic Inhibition in the Piriform Cortex. *Journal of Neuroscience* **32**:919-931 https://doi.org/10.1523/jneurosci.4112-11.2012 | PubMed

100. **Dhawale A. K.,** Hagiwara A., Bhalla U. S., Murthy V. N., Albeanu D. F. (2010) Non-redundant odor coding by sister mitral cells revealed by light addressable glomeruli in the mouse. *Nat Neurosci* **13**:1404-1412 https://doi.org/10.1038/nn.2673 | PubMed

101. **Koulakov A. A.,** Rinberg D. (2011) Sparse Incomplete Representations: A Potential Role of Olfactory Granule Cells. *Neuron* **72**:124-136 https://doi.org/10.1016/j.neuron.2011.07.031 | PubMed

102. **Lledo P.-M.,** Gheusi G., Vincent J.-D. (2005) Information Processing in the Mammalian Olfactory System. *Physiological Reviews* **85**:281-317 https://doi.org/10.1152/physrev.00008.2004 | PubMed

103. **Wachowiak M.,** Denk W., Friedrich R. W. (2004) Functional organization of sensory input to the olfactory bulb glomerulus analyzed by two-photon calcium imaging. *PNAS* **101**:9097-9102 https://doi.org/10.1073/pnas.0400438101 | PubMed

104. **Padmanabhan K.,** et al. (2016) Diverse Representations of Olfactory Information in Centrifugal Feedback Projections. *Journal of Neuroscience* **36**:7535-7545 https://doi.org/10.1523/jneurosci.3358-15.2016 | PubMed

105. **Sailor K. A.,** et al. (2016) Persistent Structural Plasticity Optimizes Sensory Information Processing in the Olfactory Bulb. *Neuron* **91**:384-396 https://doi.org/10.1016/j.neuron.2016.06.004 | PubMed

106. **Wanner A. A.,** Friedrich R. W. (2020) Whitening of odor representations by the wiring diagram of the olfactory bulb. *Nat Neurosci* **23**:433-442 https://doi.org/10.1038/s41593-019-0576-z | PubMed

107. **Willhite D. C.,** et al. (2006) Viral tracing identifies distributed columnar organization in the olfactory bulb. *Proceedings of the National Academy of Sciences* **103**:12592-12597 https://doi.org/10.1073/pnas.0602032103 | PubMed

108. **Egger V.,** Urban N. N. (2006) Dynamic connectivity in the mitral cell–granule cell microcircuit. *Seminars in Cell & Developmental Biology* **17**:424-432 https://doi.org/10.1016/j.semcdb.2006.04.006 | PubMed

109. **Schoppa N. E.,** Westbrook G. L. (2002) AMPA autoreceptors drive correlated spiking in olfactory bulb glomeruli. *Nat Neurosci* **5**:1194-1202 https://doi.org/10.1038/nn953 | PubMed

110. **Soucy E. R.,** Albeanu D. F., Fantana A. L., Murthy V. N., Meister M. (2009) Precision and diversity in an odor map on the olfactory bulb. *Nat Neurosci* **12**:210-220 https://doi.org/10.1038/nn.2262 | PubMed

111. **Luna V. M.,** Schoppa N. E. (2008) GABAergic Circuits Control Input-Spike Coupling in the Piriform Cortex. *Journal of Neuroscience* **28**:8851-8859 https://doi.org/10.1523/jneurosci.2385-08.2008 | PubMed

112. **Nunez-Parra A.,** Maurer R. K., Krahe K., Smith R. S., Araneda R. C. (2013) Disruption of centrifugal inhibition to olfactory bulb granule cells impairs olfactory discrimination. *Proc Natl Acad Sci USA* **110**:14777-14782 https://doi.org/10.1073/pnas.1310686110 | PubMed

113. **Padmanabhan K.,** et al. (2019) Centrifugal Inputs to the Main Olfactory Bulb Revealed Through Whole Brain Circuit-Mapping. *Front. Neuroanat* **12**:115 https://doi.org/10.3389/fnana.2018.00115 | PubMed

114. **Large A. M.,** Vogler N. W., Mielo S., Oswald A.-M. M. (2016) Balanced feedforward inhibition and dominant recurrent inhibition in olfactory cortex. *Proc Natl Acad Sci USA* **113**:2276-2281 https://doi.org/10.1073/pnas.1519295113 | PubMed

Peer reviews

Reviewer #1 (Public review):

Summary:

The authors build a network model of the olfactory bulb and the piriform cortex and use it to run simulations and test their hypotheses. Given the the model's settings, the authors observe drift across days in the responses to the same odors of both the mitral/tufted cells, as well as of piriform cortex neurons. When representing the M/T and PCx responses within a lower dimensional space, the apparent drift is more prominent in the PCx, while the M/T responses appear in comparison more stable. The authors further note that introducing spike-time dependent plasticity (STDP) at bulb synapses involving abGCs slows down the drift in the PCx representations, and further link this to the observation that repeated exposure to the same odorant slows down drift in the piriform cortex.

The model is clearly explained and relies on several assumptions and observations: 1) random projections of MTC from the olfactory bulb to the piriform cortex, random intra-

piriform connectivity and random piriform to bulb connectivity; 3) higher dimensionality of piriform cortex representations compared to M/T responses which enables superior decoding of odor identity in the piriform cortex; 2) spike time dependent plasticity (STDP) at synapses involving the abGCs.

The authors address an open topical problem and model is elegant in its simplicity. The authors addressed many of my concerns by plotting new analyses and by adding clarifying statements and discussion points, as well as testable predictions to the revised manuscript. In the revised manuscript, a few points remain unclear and I am listing them below for further potential discussion.

(1) Given the large in response (variability) across trials reported by Shani-Narkiss, Kay & Laurent - the question remains open: what fraction of the variability in response across days can be really accounted by adult born neurogenesis (the main topic of this study) vs. other mechanisms. I think the answer to this question is key for interpreting the results presented by the authors on the impact of adult neurogenesis on changes of mitral cell responses. Unfortunately, I could not find the answer in the revised version of the manuscript.

(2) Yamada indeed reported a "drastic reorganization of ensemble odor representation" in their manuscript (Figure 3D), but my understanding is that this was observed in the context of passive exposure to the same odor across several days in a row. This does not appear to contradict the findings of Kato et al., 2012 that when an odor is presented seldom, across days the mitral cell responses are stable. Also, data from Yamada et al. appears to show some degree of overall sparsening of odor responses in mitral cells at least at the level of a decrease in response amplitude between day 1 to day 7 of repeated passive exposure (Figure 3A, Yamada et al., 2017).

(3) There was mistake on my part on one of the papers referenced with respect to random vs. structured projections from the olfactory bulb to the piriform cortex. The one I was referring to is Chen et al., Cell, 2022 (not Chae et al., Neuron, 2022). The authors discussed the implications from the latter, while I was commenting in fact on the findings from Chen et al., 2022. This study identified structured projections of individual mitral cells along the A-P axis of the piriform cortex in conjunction with collaterals to specific subsets of extra-piriform target regions.

https://doi.org/10.7554/eLife.107905.2.sa2

Reviewer #3 (Public review):

Summary

The authors set out to explore the potential relationship between adult neurogenesis of inhibitory granule cells in the olfactory bulb and cumulative changes over days in odor-evoked spiking activity (representational drift) in the olfactory stream. They developed a richly detailed spiking neuronal network model based on Izhikevich (2003), allowing them to capture the diversity of spiking behaviors of multiple neuron types within the olfactory system. This model recapitulates the circuit organization of both the main olfactory bulb (MOB) and the piriform cortex (PCx), including connections between the two (both feedforward and corticofugal). Adult neurogenesis was captured by shuffling the weights of the model's granule cells, preserving the distribution of synaptic weights. Shuffling of granule cell connectivity resulted in cumulative changes in stimulus-evoked spiking of the model's M/T cells. Individual M/T cell tuning changed with time, and ensemble correlations dropped sharply over the temporal interval examined (long enough that almost all granule cells in the model had shuffled their weights). Interestingly, these changes in responsiveness did not disrupt low-dimensional stability of olfactory representations: when projected into a low-dimensional subspace, population vector correlations in this subspace remained elevated

across the temporal interval examined. Importantly, in the model's downstream piriform layer this was not the case. There, shuffled GC connectivity in the bulb resulted in a complete shift in piriform odor coding, including for low-dimensional projections. This is in contrast to what the model exhibited in the M/T input layer. Interestingly, these changes in PCx extended to the geometrical structure of the odor representations themselves. Finally, the authors examined the effect of experience on representational drift. Using an STDP rule, they allowed the inputs to and outputs from adult-born granule cells to change during repeated presentations of the same odor. This stabilized stimulus-evoked activity in the model's piriform layer.

Strengths

This paper suggests a link between adult neurogenesis in the olfactory bulb and representational drift in the piriform cortex. Using an elegant spiking network that faithfully recapitulates the basic physiological properties of the olfactory stream, the authors tackle a question of longstanding interest in a creative and interesting manner. As a purely theoretical study of drift, this paper presents important insights: synaptic turnover of recurrent inhibitory input can destabilize stimulus-evoked activity, but only to a degree, as representations in the bulb (the model's recurrent input layer) retain their basic geometrical form. However, this destabilized input results in profound drift in the model's second (piriform) layer, where both the tuning of individual neurons and the layer's overall functional geometry are restructured. This is a useful and important idea in the drift field and to my knowledge is novel. The bulb is not the only setting where inhibitory synapses exhibit turnover (whether through neurogenesis or synaptic dynamics), and so this exploration of the consequences of such plasticity on drift is valuable. The authors also elegantly explore a potential mechanism to stabilize representations through experience, using an STDP rule specific to the inhibitory neurons in the input layer. This has an interesting parallel with other recent theoretical work on drift in the piriform (Morales et al., 2025 PNAS), in which STDP in the piriform layer was also shown to stabilize stimulus representations there. It is fascinating to see that this same rule also stabilizes piriform representations when implemented in the bulb's granule cells.

The authors also provide a thoughtful discussion regarding differential roles of mitral and tufted cells in drift in piriform and AON and potential roles of neurogenesis in archicortex.

In general, this paper puts an important and much-needed spotlight on the role of neurogenesis and inhibitory plasticity in drift. In this light, it is a valuable and exciting contribution to the drift conversation.

Comments on revisions:

I appreciate the substantial revisions the authors have made to the manuscript. The paper is clearly improved and addresses an important and timely question: the relationship between adult neurogenesis and drift. In particular, the effort to link adult neurogenesis in the olfactory bulb to the long-term stability of odor representations downstream is valuable, and the modeling provides useful mechanistic intuition about how inhibitory circuit remodeling could influence representational drift across layers.

That said, I remain concerned that the manuscript, as currently framed, risks giving readers the incorrect impression that experimental work has established progressive, time-dependent drift in the odor tuning of olfactory bulb neurons. Experimental studies do show that ongoing experience with a set of odors can profoundly alter bulbar responses to those odors, but longitudinal measurements in which the tested odors are not repeatedly presented between sessions have instead emphasized remarkable stability of mitral/tufted tuning over days to months across multiple groups. I also think it would strengthen the manuscript to avoid anchoring the empirical comparison too heavily on a single paradigm (Yamada et al.,

2017). The experimental literature spans multiple regimes, including daily odor exposure with ongoing experience and longitudinal measurements in which the tested odors are not repeatedly presented between sessions, and these regimes can yield qualitatively different degrees of reorganization. Situating the model explicitly within this broader landscape, rather than emphasizing one dataset, would make the interpretation clearer and prevent readers from overgeneralizing the Yamada findings to baseline bulbar stability. This distinction is especially important because it contrasts with what has been reported in piriform cortex, where representational drift is observed even in the absence of ongoing experience with a given odor set, and where repeated daily encounters with the same odors can slow or arrest that drift.

https://doi.org/10.7554/eLife.107905.2.sa1

Author response:

The following is the authors' response to the original reviews.

We thank the editor and reviewers for their thoughtful and constructive feedback. We appreciate that all reviewers recognized the value of our study in linking adult neurogenesis and synaptic plasticity to representational drift in the olfactory system. They described the model as elegant and well-motivated, and agreed that it provides new theoretical insight into how stability and adaptability can coexist in sensory representations. The reviewers also identified areas where our manuscript could be strengthened, and as outlined in our revision plan we have:

(1) Refined our description of mitral/tufted cell stability and expand on within-session and across-day variability.

(2) Substantially expanded the Discussion to compare our modeling assumptions with experimental findings and recent anatomical evidence. Additionally, we have included the limitations of the study and areas for future investigation.

(3) Included a clearer description of the STDP implementation, plastic synapses, and their functional effects.

(4) Add a short section outlining model-based predictions that can guide future experiments. We also made minor textual edits to improve precision and flow, including citing prior conceptual work and clarifying model procedures.

These changes have strengthened both the conceptual framing and technical clarity of the paper. We are grateful for the reviewers' careful reading and valuable suggestions.

> ***Public Reviews:***
>
> ***Reviewer #1 (Public review):***
>
> *Summary:*
>
> *The authors build a network model of the olfactory bulb and the piriform cortex and use it to run simulations and test their hypotheses. Given the model's settings, the authors observe drift across days in the responses to the same odors of both the mitral/tufted cells, as well as of piriform cortex neurons. When representing the M/T and PCx responses within a lower-dimensional space, the apparent drift is more prominent in the PCx, while the M/T responses appear in comparison more stable. The authors further note that introducing spike-time dependent plasticity (STDP) at bulb synapses involving abGCs slows down the drift in the PCx representations, and further link this to the*

> *observation that repeated exposure to the same odorant slows down drift in the piriform cortex.*
>
> *The model is clearly explained and relies on several assumptions and observations:*
>
> *(1) Random projections of MTC from the olfactory bulb to the piriform cortex, random intra-piriform connectivity, and random piriform to bulb connectivity.*
>
> *(2) Higher dimensionality of piriform cortex representations compared to M/T responses, which enables superior decoding of odor identity in the piriform cortex.*
>
> *(3) Spike time-dependent plasticity (STDP) at synapses involving the abGCs.*
>
> *The authors address an open topical problem, and the model is elegant in its simplicity. I have however, several major concerns with the hypotheses underlying the model and with its biological plausibility.*
>
> *Concerns:*
>
> *(1) In their model, the authors propose that MTC remain stable at the population level, despite changes in individual MTC responses.*
>
> *The authors cite several experimental studies to support their claims that individual MTC responses to the same odors change (some increase, some decrease) across days. Interpreting the results of these studies must, however, take into account the variability of M/T responses across odor presentation repeats within the same session vs. across sessions. In the Shani-Narkiss et al., Frontiers in Neural Circuits, 2023 study referenced, a large fraction of the variability across days in M/T responses is also observed across repeats to the same odorant in the same session (Shani-Narkiss et al., Figure 4), while the authors have M/T responses in the same session that are highly reproducible. This is an important point to consider and address, since it constrains how much of the variability in M/T responses can be attributed to adult neurogenesis in the olfactory bulb versus to other networks' inhibitory mechanisms, which do not rely on neurogenesis. In the authors' model, the variability in M/T responses observed across days emerges as a result of adult-born neurogenesis, which does not need to be the main source of variability observed in imaging experiments (Shani-Narkiss et al., Figure 4).*

We agree with the reviewer and believe this is a critical discussion point. Indeed, both in Shani-Narkiss et al, Kay and Laurent, 1999, and in our lab, we observe trial-to-trial variability that occurs in the same recording session; as the reviewer correctly points out, this cannot be due to neurogenesis. These fluctuations may be trial to-trial noise, or reflect dynamics associated with other behaviors such as running (Chockanathan, et al. 2021) and decision making (Kay and Laurent, 1999). There is growing repertoire of literature showing that neural variability in early sensory coding appears to depend on behavioral fluctuations and internal states (Niell and Stryker for example). This variability that happens within a session in the Shani-Narkiss et al work may reflect some of these behaviorally relevant features of early olfactory coding, something that our model cannot account for. This is an excellent discussion point and we have included text (line 153-157, and line 321-330) in the manuscript to note this aspect of the data and how one can think of it in the context of our results.

> *Another study (Kato et al., Neuron, 2012, Figure 4) reported that mitral cell responses to odors experienced repeatedly across 7 days tend to sparsen and decrease in amplitude systematically, while mitral cell responses to the same odor on day 1 vs. day 7 when the odor is not presented repeatedly in between seem less affected (although the authors also reported a decrease in the CI for this condition). As such, Kato et al. mostly report decreases in mitral cell odor responses with repeated odor exposure at both the*

> *individual and population level, and not so much increases and decreases in the individual mitral cell responses, and stability at the population level.*

Thank you for raising this important point regarding the findings of Kato et al. (2012). We agree that their results suggest increased sparsening and stability in M/T cell odor responses with repeated exposure. However, as noted in Yamada et al. (2017), the experimental literature on this question remains mixed. Yamada and colleagues reported a "drastic reorganization of ensemble odor representation" across days and emphasized that "sensory experience does not necessarily cause a major sparsening of the odor response," explicitly contrasting their findings with those of Kato et al. (2012).

Our model captures the dynamics observed in Yamada et al. (2017), providing a mechanistic explanation for how significant reorganization can emerge in M/T ensembles despite stable low-dimensional population structure. In both Yamada et al (2017) and Kato et al (2012) the investigators have nuanced differences in experimental design (method of head fixation, behavioral paradigm used, training etc.), all of which are known to affect olfactory responses and therefore the degree of sparsity and overlap in population codes. Our model does not include any of these behavioral features that may differentially engage the olfactory circuit and thus affect population responses. Notably, in previous work, we highlight how even simple changes to top down feedback that reflect one phenomenological manipulation to functional connectivity in the olfactory circuit could have disparate effects on the degree of sparsity in neural representations over time whereby this manipulation would be activated by some behavior broadly. In our current model, there is no behavior that would allow us to study the critical features of the neural activity code in the M/T cells. Instead we focus on one specific aspect, adult neurogenesis which we can explicitly manipulate and affect in a biologically meaningful way. The review's point however is well taken and important, and we have added text to the Discussion (line 336-344) to highlight the differing experimental outcomes and to clarify how our model aligns with the Yamada et al. results.

> *(2) In Figure 1, a set of GCs is killed off, and new GCs are integrated in the network as abGC. Following the elimination of 10% of GCs in the network, new cells are added and randomly assigned synaptic weights between these abGCs and MTC, GCs, SACs, and top-down projections from PCx. This is done for 11 days, during which time all GCs have gone through adult neurogenesis.*
>
> *Is the authors' assumption here that across the 11 days, all GCs are being replaced? This seems to depart from the known biology of the olfactory bulb granule cells, i.e., GCs survive for a large fraction of the animal's life.*

Thank you for raising this important point regarding the lifespan of granule cells (GCs). We agree that developmentally born GCs are not fully replaced. Indeed, multiple studies indicate that some developmentally born GCs can survive for very long periods, up to 18-24 months, essentially the lifetime of the animal (Kaplan, 1985; Petreanu & Alvarez-Buylla, 2002). However, the fraction of total GCs that such long lived GCs constitute remains an open question, in part because of challenges to measure the lifetime survival of newborn neurons. What there is consensus on is the significant size of the granule-cell population undergoing continuous turnover through adult neurogenesis (reviewed in Lepousez et al., 2013).

We should clarify that we do not assume that 100% of the granule cell population turns over in an 11 day period. We use "day" to represent a static epoch over which we can implement plasticity rules across two time scales. Critically, we also randomize the turnover treating every cell in the GC population as equally likely to be replaced. Prior experimental evidence suggests that some GCs are more likely to persist (possibly as a result of experience, Magavi et al., 2005) which may in some regards make our result on stabilization following repeated sensory exposure more dramatic (as the GCs that show the largest change following STDP may also be the ones that are the most stable, and therefore least likely to turnover). We do

not include this in our model as we could not identify a framework for "selecting" which GCs would persist that would not be tautological. The point the reviewer raises is critical, and a discussion of these points is warranted - which we now include in the manuscript (line 352-361).

Additionally, there is some evidence that behaviors, such as novelty, can increase the rate of adult neurogenesis (Kamimura et al., 2022, H.van Praag et al.,1999, Gheusi and Lledo., 2014) , suggesting a complex reciprocal relationship between the mechanisms that generate the cells shaping how olfactory stimuli are encoded for and the encoding process itself; our model also does not include any of these dynamic features which represent an additional layer of complexity, which may further provide an intermediate time scale, one of behavioral selection and action, that is slower than the milliseconds on which spike time dependent plasticity happens, but faster than the time scale of neurogenesis. We include this point in the discussion also (line 352-361).

Our 11-day simulation however is designed to uncover how plasticity across multiple timescales (STDP and adult neurogenesis) at the network level shapes odor representations as multiple rounds of GC turnover occur. Changing the timescale and magnitude replacement in the simulations (either in terms of days or percent cells replaced) would affect the degree to which drift happens, but not phenomenon. Additionally, the representational structure in our model at intermediate time points (e.g., days 8~10) would correspond well to scenarios in which some fraction of developmentally born GCs persists in the circuit. Thus, our simulations span a range of possible empirical regimes, from high turnover to partial preservation. We have added discussion to the revised manuscript (line 352-361) clarifying this point and acknowledging the biological heterogeneity in GC lifespans.

> *(3) The authors' model relies on several key assumptions: random projections of MTC from the olfactory bulb to the piriform cortex, random intra-piriform connectivity, and random piriform to bulb connectivity. These assumptions are not necessarily accurate, as recent work revealed structure in the projections from the olfactory bulb to the piriform cortex and structure within the piriform cortex connectivity itself (Fink et al., bioRxiv, 2025; Chae et al., Cell, 2022; Zeppilli et al., eLife, 2021).*
>
> *How do the results of the model relating adult neurogenesis in the bulb to drift in the piriform cortex representations change when considering an alternative scenario in which the olfactory bulb to piriform and intra-piriform connectivity is not fully distributed and indistinguishable from random, but rather is structured?*

Thank you for pointing us to these important studies. We fully agree with the reviewer that the structure of the olfactory system might not be purely random, but we do not believe these papers contradict the level of abstraction used in our model.

Zeppilli et al. (2021) map molecularly defined projection neuron subtypes and their preferential targeting of different cortical and subcortical regions, but they do not report any fine-scale topographic organization of bulb → piriform connectivity that would contradict a view of randomly distributed input to piriform cortex. Studies from our lab using retrograde tracers in the blub show some spatial clustering of piriform cortical neurons whose axons project to the bulb (Padmanabhan et al., 2016, 2019), but these studies do not identify any "functional organization" or structure. Chae et al., (2022) focus on distinct long-range functional loops (mitral ↔ piriform vs tufted ↔ AON) and the differential role of cortical feedback, but again, at the level of cortical regions rather than individual cells and connectivity. Notably, our model does not consider AON.

Finally, Fink et al. (2025) reports a "like-to-like" excitatory connectivity motif within the piriform cortex and an experience-dependent reorganization of inhibitory synapses. As the authors note, "... this like-to-like motif is unlikely to reflect common input from the olfactory

bulb", so it does not conflict with our assumption of broadly random bulb → piriform input. This "like-to-like" motif is reflected in our model by wiring a certain subpopulation of piriform cells. On the other hand, we agree that the experience dependent changes in inhibitory connectivity within PCx are highly relevant for learning related plasticity but fall outside the scope of our study. We intentionally omitted piriform plasticity to isolate the contributions of adult neurogenesis in the bulb and plasticity acting on adult-born granule cells. But incorporating such cortical plasticity is an important direction for future work. We added a discussion (line 395-405) on this important point raised by the reviewer in the revised manuscript.

> *(4) I didn't understand the logic of the low-dimensional space analysis for M/T cells and piriform cortex neurons (Figures 2 & 3). In the authors' model, the full-ensemble M/T responses are reorganized over time, presumably due to the adult-born neurogenesis. Analyzing a lower-dimensional projection of the ensemble trajectories reveals a lower degree of re-organization. This is the same for the piriform cortex, but relatively, the piriform ensembles displayed in a low-dimensional embedding appear to drift more compared to the M/T ensembles.*
>
> *This analysis triggers a few questions: which representation is relevant for the brain function - the high or the low-dimensional projection? What fraction of response variance is included in the low-dimensional space analysis? How did the authors decide the low-dimensional cut-off? Why does STDP cause more drift in piriform cortex ensembles vs. M/T ensembles? Is this because of the assumed higher dimensionality of the piriform cortex representations compared to the mitral cells?*

Thank you for these thoughtful questions. We clarify the logic and purpose of the low-dimensional analyses and address each point below.

(1) Which representation is relevant for brain function, the high-dimensional or low-dimensional one?

We believe both representations are meaningful, with each capturing different aspects of the neural code. The high-dimensional activity reflects the full variability of individual cell responses, while the low-dimensional projection captures the dominant population level components that downstream areas are most likely to use for readout. We found that the low-dimensional representations are more stable in the bulb than in PCx, suggesting that information is used differentially between the two areas. The bulb provides a stable, sensory-anchored population code that reliably represents odor identity over time, consistent with both electrophysiological and behavioral studies (Nagayama et al., 2004, Chen et al., 2009, Davison and Katz, 2007, Cavaretta et al., 2018). This is consistent with its role as the first stage of information processing in the olfactory system which provides faithful representations that downstream circuits receive. The piriform cortex, by contrast, transforms this stable input into a more flexible representation. Drift in its low-dimensional space may reflect ongoing plasticity (Schoonover et al., Nature, 2021), integration of contextual signals, or higherdimensional computations characteristic of PCx (Fink et al., bioRxiv, 2025), suggesting its role more as an associative cortex instead of a pure sensory cortex.

(2) What fraction of variance is included in the low-dimensional space, and how was the cutoff chosen?

In our simulations, these PCs captured the majority of variance relevant for odor identity (~60–70% for M/T cells and ~55–65% for piriform cortex). We now report these fractions explicitly in Methods (line 937-939).

(3) Why does STDP cause more drift in piriform-cortex ensembles than in M/T ensembles? Does this reflect higher dimensionality in piriform cortex?

In our model, STDP does not cause more drift in PCx. It actually reduces drift and stabilizes PCx representations relative to the condition without STDP (as shown in Fig. 4C2). STDP has a much smaller effect in the bulb because: (1) M/T cells continue to receive stable odor input from the glomeruli and (2) the low-dimensional M/T representation is already stable even without plasticity. We have edited the manuscript to reiterate this point in both the results and discussion.

The reviewer is correct that the piriform cortex naturally exhibits more drift than the bulb, and their comment that this is due to its substantially higher representational dimensionality is spot on. The PCx contains many more neurons, receives highly divergent OB → PCx inputs, and has dense recurrent connectivity, all of which create many more degrees of freedom through which representations can drift. Additionally, because individual PCx neurons are sampling from a substantially more diverse combinatorial space of inputs (include feedback to piriform from an array of regions, Illig, 2005, Majak et al., 2004, Chapuis et al., 2013), the "dimensionality" of the population code is likely higher dimensional. While STDP stabilizes the dimensions of the PCx representation that are reinforced during plasticity, due to the large number of orthogonal dimensions available, some residual drift remains. Additionally, as the reviewer notes, there are some forms of plasticity, such as inhibitory plasticity in PCx that are not included in the model, that may also have an impact on both the representations, and the underlying dimensionality of those representations. We include these points in the discussion (line 381-394).

> *(5) Could the authors comment whether STDP at abGC synapses and its impact on decreasing drift represent a new insight, and also put it into context? Several studies (e.g., Lledo, Murthy, Komiyama groups) reported that abGC integrates in the network in an activity-dependent manner, and not randomly, and as such stabilizes the active neuronal responses, which is consistent with the authors' report.*
>
> *Related, I couldn't find through the manuscript which synapses involving abGCs they focus on, or what is the relative contribution of the various plastic synapses shown in the cartoon from Figure 4 A1 (circles and triangles).*

We thank the reviewer for raising this question. As the reviewer pointed out, several studies have shown that abGCs integrate into the bulb circuit in an activity dependent manner. They preferentially form synapses onto mitral/tufted cells that respond to behaviorally important odors, this "selection of surviving cells" is not included in our model. Instead, we use STDP at the synaptic level. This is of course not analogous, but provides a computational framework wherein the selection of surviving abGCs could be incorporated in future studies. It is perhaps notable that in our large scale simulations, synaptic changes at the population level may reflect some of this activity-dependent selection.

To that end, our model provides a new insight and suggests a broader function for adult neurogenesis. For example, when certain odors are reinforced in an activity dependent manner, abGCs born during that period may stabilize the circuits that respond to those odors. The resulting reduction of drift would help keep the representation of those odors stable over time, even while other parts of the circuit continue to change. We now highlight this idea in the Discussion (line 366-373).

For the second part of the question: in our model, STDP acts on two sets of connections. It applies to the synapses onto abGCs from M/T cells, GC/SAC cells, and PCx neurons. It also applies to the synapses that abGCs project to, including those onto M/T cells and GC/SAC cells. We have clarified this in the revised Methods (line 10011004).

> *(6) The study would be strengthened, in my opinion, by including specific testable predictions that the authors' models make, which can be further food for thought for experimentalists.*
>
> *How does suppression of adult-born neurogenesis in the OB impact the stability of mitral cell odor responses? How about piriform cortex ensembles?*

We appreciate the reviewer's suggestion and formalize the following two predictions from our model:

Prediction 1: Suppressing adult neurogenesis will reduce spontaneous representational drift in the PCx. Increasing spike-timing-dependent plasticity during periods of experience with a specific odor will selectively stabilize representations of that odor.

Prediction 2: Adult neurogenesis will not affect AON representations of odor identity or concentration in the same way that PCx representations are altered and drift.

We include these two ideas in the discussion as experimentally testable predictions.

> ***Reviewer #2 (Public review):***
>
> *Summary:*
>
> *The authors address a critical problem in olfactory coding. It has long been known that adult neurogenesis, specifically in the form of adult-born granule cells that embed into the existing inhibitory networks on the olfactory bulb, can potentially alter the responses of Mitral/Tufted neurons that project activity to the Piriform Cortex and to other areas of the brain. Fundamentally, it would seem that these granule cells could alter the stability of neural codes in the OB over time. The authors develop a spiking network model to explore how stability can be achieved both in the OB over time and in the PC, which receives inputs. The model recapitulates published activity recordings of M/T cells and shows how activity in different M/T cells from the same glomerulus shifts over time in ways that, in spite of the shift, preserve population/glomerular level codes. However, these different M/T cells fan out onto different pyramidal cells of the PC, which gives rise to instability at that level. STDP then, is necessary to maintain stability at the PC level as long as odor environments remain constant. These results may also apply to a similar neurogenesis-based change in the Dentate Gyrus, which generates instability in CA1/3 regions of the hippocampus*
>
> *Strengths:*
>
> *A robust network model that untangles important, seemingly contradictory mechanisms that underlie olfactory coding.*
>
> *Weaknesses:*
>
> *The work is a significant contribution to understanding olfactory coding. But the manuscript would benefit from a brief discussion of why neurogenesis occurs in the first place - e.g., injury, ongoing needs for plasticity, and adapting to turnover of ORNs. There is literature on this topic. It seems counterintuitive to have a process in the MOB (and for that matter in the DG) that potentially disrupts the ability to generate stable codes both in the MOB and PC, and in particular a disruption that requires two different mechanisms - multiple M/T cells per glomerulus in the MOB and STDP in the PC - to counteract.*

We appreciate the reviewer's suggestion and added discussion on this point in the revised manuscript (line 431-435).

> *Given that neurogenesis has an important function, and a mechanism is in place to compensate for it in the MOB, why would it then be disrupted in fan-out projections to the PC? The answer may lie in the need for fan-out projections so that pyramidal neurons in the PC can combinatorially represent many different inputs from the MOB. So something like STDP would be needed to maintain stability in the face of the need for this coding strategy.*
>
> *This kind of discussion, or something like it, would help readers understand why these mechanisms occur in the first place. It is interesting that PC stability requires that odor environments be stable, and that this stability drives PC representational stability. This result suggests experimental work to test this hypothesis. As such, it is a novel outcome of the research.*

We agree with the reviewer. The fan-out from the bulb to the piriform cortex is essential for the combinatorial coding that allows PCx neurons to represent many odor features and mixtures. This architecture gives the piriform cortex great coding capacity, but it also makes the system sensitive to small changes in its inputs. As a result, drift that originates in the bulb can spread more easily in PCx. A stabilizing mechanism is therefore needed downstream. In our model, STDP provides this stabilization by reinforcing the dimensions that carry meaningful odor structure. This allows the piriform cortex to keep a stable population code even when its inputs change over time. Neurogenesis supplies the flexibility, the fan-out supplies the expressive power, and STDP supplies the stability. All three elements work together to support a system that must recognize odors reliably while still adapting to new sensory experiences. We have added discussion on this point in the revised manuscript (line 395-405).

> ***Reviewer #3 (Public review):***
>
> *Summary*
>
> *The authors set out to explore the potential relationship between adult neurogenesis of inhibitory granule cells in the olfactory bulb and cumulative changes over days in odorevoked spiking activity (representational drift) in the olfactory stream. They developed a richly detailed spiking neuronal network model based on Izhikevich (2003), allowing them to capture the diversity of spiking behaviors of multiple neuron types within the olfactory system. This model recapitulates the circuit organization of both the main olfactory bulb (MOB) and the piriform cortex (PCx), including connections between the two (both feedforward and corticofugal). Adult neurogenesis was captured by shuffling the weights of the model's granule cells, preserving the distribution of synaptic weights. Shuffling of granule cell connectivity resulted in cumulative changes in stimulus-evoked spiking of the model's M/T cells. Individual M/T cell tuning changed with time, and ensemble correlations dropped sharply over the temporal interval examined (long enough that almost all granule cells in the model had shuffled their weights).*
>
> *Interestingly, these changes in responsiveness did not disrupt low-dimensional stability of olfactory representations: when projected into a low-dimensional subspace, population vector correlations in this subspace remained elevated across the temporal interval examined. Importantly, in the model's downstream piriform layer, this was not the case. There, shuffled GC connectivity in the bulb resulted in a complete shift in piriform odor coding, including for low-dimensional projections. This is in contrast to what the model exhibited in the M/T input layer. Interestingly, these changes in PCx extended to the geometrical structure of the odor representations themselves. Finally, the authors examined the effect of experience on representational drift. Using an STDP rule, they allowed the inputs to and outputs from adult-born granule cells to change during*

> *repeated presentations of the same odor. This stabilized stimulus-evoked activity in the model's piriform layer.*
>
> *Strengths*
>
> *This paper suggests a link between adult neurogenesis in the olfactory bulb and representational drift in the piriform cortex. Using an elegant spiking network that faithfully recapitulates the basic physiological properties of the olfactory stream, the authors tackle a question of longstanding interest in a creative and interesting manner. As a purely theoretical study of drift, this paper presents important insights: synaptic turnover of recurrent inhibitory input can destabilize stimulus-evoked activity, but only to a degree, as representations in the bulb (the model's recurrent input layer) retain their basic geometrical form. However, this destabilized input results in profound drift in the model's second (piriform) layer, where both the tuning of individual neurons and the layer's overall functional geometry are restructured. This is a useful and important idea in the drift field, and to my knowledge, it is novel. The bulb is not the only setting where inhibitory synapses exhibit turnover (whether through neurogenesis or synaptic dynamics), and so this exploration of the consequences of such plasticity on drift is valuable. The authors also elegantly explore a potential mechanism to stabilize representations through experience, using an STDP rule specific to the inhibitory neurons in the input layer. This has an interesting parallel with other recent theoretical work on drift in the piriform (Morales et al., 2025 PNAS), in which STDP in the piriform layer was also shown to stabilize stimulus representations there. It is fascinating to see that this same rule also stabilizes piriform representations when implemented in the bulb's granule cells.*
>
> *The authors also provide a thoughtful discussion regarding the differential roles of mitral and tufted cells in drift in piriform and AON and the potential roles of neurogenesis in archicortex.*
>
> *In general, this paper puts an important and much-needed spotlight on the role of neurogenesis and inhibitory plasticity in drift. In this light, it is a valuable and exciting contribution to the drift conversation.*

We appreciate the reviewer's comment and thank them for their thoughtful feedback.

> *Weaknesses*
>
> *I have one major, general concern that I think must be addressed to permit proper interpretation of the results.*
>
> *I worry that the authors' model may confuse thinking on drift in the olfactory system, because of differences in the behavior of their model from known features of the olfactory bulb. In their model, the tuning of individual bulbar neurons drifts over time.*
>
> *This is inconsistent with the experimental literature on the stability of odor-evoked activity in the olfactory bulb.*
>
> *In a foundational paper, Bhalla & Bower (1997) recorded from mitral and tufted cells in the olfactory bulb of freely moving rats and measured the odor tuning of well-isolated single units across a five-day interval. They found that the tuning of a single cell was quite variable within a day, across trials, but that this variability did not increase with time. Indeed, their measure of response similarity was equivalent within and across days. In what now reads as a prescient anticipation of the drift phenomenon, Bhalla and Bower concluded: "it is clear, at least over five days, that the cell is bounded in how it can respond. If this were not the case, we would expect a continual increase in relative response variability over multiple days (the equivalent of response drift). Instead, the*

> *degree of variability in the responses of single cells is stable over the length of time we have recorded." Thus, even at the level of single cells, this early paper argues that the bulb is stable.*
>
> *This basic result has since been replicated by several groups. Kato et al. (2012) used chronic two-photon calcium imaging of mitral cells in awake, head-fixed mice and likewise found that, while odor responses could be modulated by recent experience (odor exposure leading to transient adaptation), the underlying tuning of individual cells remained stable. While experience altered mitral cell odor responses, those responses recovered to their original form at the level of the single neuron, maintaining tuning over extended periods (two months). More recently, the Mizrahi lab (Shani-Narkiss et al., 2023) extended chronic imaging to six months, reporting that single-cell odor tuning curves remained highly similar over this period. These studies reinforce Bhalla and Bower's original conclusion: despite trial-to-trial variability, olfactory bulb neurons maintain stable odor tuning across extended timescales, with plasticity emerging primarily in response to experience. (The Yamada et al., 2017 paper, which the authors here cite, is not an appropriate comparison. In Yamada, mice were exposed daily to odor. Therefore, the changes observed in Yamada are a function of odor experience, not of time alone. Yamada does not include data in which the tuning of bulb neurons is measured in the absence of intervening experience.)*
>
> *Therefore, a model that relies on instability in the tuning of bulbar neurons risks giving the incorrect impression that the bulb drifts over time. This difference should be explicitly addressed by the authors to avoid any potential confusion. Perhaps the best course of action would be to fit their model to Mizrahi's data, should this data be available, and see if, when constrained by empirical observation, the model still produces drift in piriform. If so, this would dramatically strengthen the paper. If this is not feasible, then I suggest being very explicit about this difference between the behavior of the model and what has been shown empirically. I appreciate that in the data there is modest drift (e.g., Shani-Narkiss' Figure 8C), but the changes reported there really are modest compared to what is exhibited by the model. A compromise would be to simply apply these metrics to the model and match the model's similarity to the Shani-Narkiss data. Then the authors could ask what effect this has on drift in piriform.*
>
> *The risk here is that people will conclude from this paper that drift in piriform may simply be inherited from instability in the bulb. This view is inconsistent with what has been documented empirically, and so great care is warranted to avoid conveying that impression to the community.*

We thank the reviewer for highlighting this important issue. We agree that the interpretation of our model requires care to avoid implying that the olfactory bulb exhibits spontaneous drift. As the reviewer points out, the empirical literature shows that M/T-cell tuning is highly stable for infrequently experienced odors, but can change with daily, persistent odor exposure (e.g., Kato et al., 2012; Yamada et al., 2017).

We thank the reviewer for highlighting the Bhalla and Bower paper, as it is foundational and actually raises a number of interesting and important points. As the authors noted, there was significant variability in trial-to-trial responses over sessions and days in single neurons. This is likely due to on-going dynamics (Laurent, 1999), the impact of behaviorally relevant top-down feedback (Chen and Padmanabhan, 2022), decision making (Kay and Laurent, 1999), and an array of factors that our model does not include. In that manuscript, the authors note “the variability of the same neuron recorded over different days…was not statistically different from the within day comparisons.” While these results appear *prima facie* to be different from our results, there are several reasons why they may not be the case.

First, different metrics are used for measuring neuronal stability, which may contribute to some of the differences. Second, and perhaps more importantly and interestingly, the authors in that study noted the significant trial-to-trial variability within day, which is not present in our study because our model has none of the richness of behavior that Bhalla and Bower found in the freely behaving rat. This variability within day (which is much higher than what we report) would reduce the impact of drift across days - a result that would complicate how plasticity across multiple timescales occurs. We thank the reviewer for the insights on this critical study and include these points in our discussion (line 321-330).

Neural responses to odor representations are incredibly variable across different time scales (Padmanabhan and Urban 2010, Angelo et al 2011, Kapoor and Urban 2006, Friedrich and Laurent, 2001, Smear et al 2011, Wesson et al 2008). In our model, none of this selection of survival related to behavior is included, nor are there specific rules about which synapses may be preferentially strengthened (due to neuro modulation corresponding to behavioral choice and reinforcement learning). Instead, we aimed to recapitulate the experimental design of a few studies (Kato et al 2012, Yamada et al, 2017) to understand how neurogenesis and drift are related. Over the simulated 10 days, the odor is presented every day, and the network is otherwise frozen between sessions—meaning the model lacks mechanisms that would normally support recovery during intervals without odor exposure. Under these conditions, adult neurogenesis effectively interacts with repeated experience, producing gradual changes in individual M/T-cell tuning. Thus, our results should be interpreted as modeling experience dependent changes over the timescale of neurogenesis, not as evidence for spontaneous drift in the bulb. We now state this explicitly in the Discussion to prevent confusion and expand the discussion to incorporate some of these critical ideas (line 321-330).

> *Major comments (all related to the above point)*
>
> *(1) Lines 146-168: The authors find in their model that "individual M/T cells changed their responses to the same odor across days due to adult-neurogenesis, with some cells decreasing the firing rate responses (Fig.2A1 top) while other cells increased the magnitude of their responses (Fig. 2A2 bottom, Fig. S2)" they also report a significant decrease in the "full ensemble correlation" in their model over time. They claim that these changes in individual cell tuning are "similar to what has been observed by others using calcium imaging of M/T cell activity (Kato et al., 2012 and Yamada et al., 2017)" and that the decrease in full ensemble correlation is "consistent with experimental observations (Yamada et al., 2017)." However, the conditions of the Kato and Yamada experiments that demonstrate response change are not comparable here, as odors were presented daily to the animals in these experiments. Therefore, the changes in odor tuning found in the Kato and Yamada papers (Kato Figure 4D; Yamada Figure 3E) are a function of accumulated experience with odor. This distinction is crucial because experience-induced changes reflect an underlying learning process, whereas changes that simply accumulate over time are more consistent with drift. The conditions of their model are more similar to those employed in other experiments described in Kato et al. 2012 (Figure 6C) as well as Shani-Narkiss et al. (2023), in which bulb tuning is measured not as a function of intervening experience, but rather as a function of time (Kato's "recovery" experiment). What is found in Kato is that even across two months, the tuning of individual mitral cells is stable. What alters tuning is experience with odor, the core finding of both the Kato et al., 2012 paper and also Yamada et al., 2017. It is crucial that this is clarified in the text.*

We thank the reviewer. As the issue raised here is related to the previous comment, we have clarified this in the revised text to avoid any misleading comparison and specify what aspects of our computational model map onto experimental studies and what aspects we cannot recapitulate and as a result, the places where our comparisons are limited.

> *(2) The authors show that in a reduced-space correlation metric, the correlation of lowdimensional trajectories "remained high across all days"..."consistent with a recent experimental study" (Shani-Narkiss et al., 2023). It is true that in the Shani-Narkiss paper, a consistent low-dimensional response is found across days (t-SNE analysis in Shani-Narkiss Figure 7B). However, the key difference between the Shani-Narkiss data and the results reported here is that Shani-Narkiss also observed relative stability in the native space (Shani-Narkiss Figure 8). They conclude that they "find a relatively stable response of single neurons to odors in either awake or anesthetized states and a relatively stable representation of odors by the MC population as a whole (Figures 6-8; Bhalla and Bower, 1997)." This should be better clarified in the text.*

We agree with the reviewer that some of the cells in Shani-Narkiss Figure 8B showed relatively stable responses (while others did not). However, there is a clear monotonic increase in the “Average differences” over time, from “Same day” to “1 month” to “6 month”, as quantified in their Figure 8B. Although the author concluded that they "find a relatively stable response of single neurons”, we would argue that their data also provided evidence for what we would term “relatively unstable responses” as found in our model. But per reviewer’s suggestion, we better clarify it in the text now (line 194197).

> *(3) In the discussion, the authors state that "In the MOB, individual M/T cells exhibited variable odor responses akin to gain control, altering their firing rate magnitudes over time. This is consistent with earlier experimental studies using calcium-imaging." (L3146). Again, I disagree that these data are consistent with what has been published thus far. Changes in gain would have resulted in increased variability across days in the Bhalla data. Moreover, changes in gain would be captured by Kato's change index ("To quantify the changes in mitral cell responses, we calculated the change index (CI) for each responsive mitral cell-odor pair on each trial (trial X) of a given day as (response on trial X - the initial response on day 1)/(response on trial X + the initial response on day 1). Thus, CI ranges from −1 to 1, where a value of −1 represents a complete loss of response, 1 represents the emergence of a new response, and 0 represents no change." Kato et al.). This index will capture changes in gain. However, as shown in Figure 4D (red traces), Figure 6C (Recovery and Odor set B during odor set A experience and vice versa), the change index is either zero or near zero. If the authors wish to claim that their model is consistent with these data, they should also compute Kato's change index for M/T odor-cell pairs in their model and show that it also remains at 0 over time, absent experience.*

We appreciate the reviewer’s suggestion and edited the text to make it more accurate (line 319-320).

> ***Recommendations for the authors:***
>
> ***Reviewer #3 (Recommendations for the authors):***
>
> *(1) Line 28 "a graduate alteration in sensory perception". We do not know if drift results in changes in perception. If anything, behavioral evidence suggests that perception remains stable in spite of drift. For example, in Driscoll et al. (2017) mice are able to successfully navigate a virtual T maze despite drift, and in Schoonover et al. (2021), mice maintain aversive responses following fear conditioning, despite drift in the piriform. Finally, spatial navigation appears unimpaired despite pronounced drift in the hippocampus (e.g., Climer et al., 2025). It would be more appropriate to say "stimulusevoked activity patterns" than "sensory perception" or other words that refer to neuronal activity rather than cognition or behavior.*

We edited the text to make it more accurate per the reviewer’s suggestion (line 27).

> *(2) In the introduction, the authors state: "This representational drift has led to the hypothesis that PCx, rather than being a primary sensory area, may be more like an association cortical region." (L76-78). However, the hypothesis that PCx operates as an association cortex comes originally from Haberly's work and thinking (e.g., Haberly and Bower, 1984, elaborated in extensive detail in Haberly, 2001). I think it would be appropriate to acknowledge that here.*

We added the references to make acknowledge that per the reviewer's suggestion (line 77).

> *(3) In the methods, the authors elegantly describe how they induce neurogenesis in their model using weight reshuffling (L805-814). I think it could really help the reader understand the model if this idea were also included in the results section. As the results section currently reads, it seems as if their model implemented neurogenesis in a different fashion: "To do this, following elimination of 10% of the GCs in the network, we added new cells and randomly assigned synaptic weights between these abGCs and M/Ts". I appreciate that in their model, shuffling all the weights of a given GC randomly is akin to "elimination", but I feel like at first blush the results section risks giving an impression a bit different than that actually used in the model.*

We edited the text to make it more accurate per the reviewer's suggestion (line 110-112).

https://doi.org/10.7554/eLife.107905.2.sa0